Matching next-to-leading-order and high-energy-resummed calculations of heavy-quarkonium-hadroproduction cross sections

Jean-Philippe Lansberg,[a] **Maxim Nefedov**[a,b,1] **and Melih A. Ozcelik**[a,c]

[a]*Université Paris-Saclay, CNRS, IJCLab,*
91405 Orsay, France

[b]*National Centre for Nuclear Research (NCBJ),*
Pasteura 7, 02-093 Warsaw, Poland

[c]*Institute for Theoretical Particle Physics, KIT,*
76128 Karlsruhe, Germany

E-mail: Jean-Philippe.Lansberg@in2p3.fr, maxim.nefedov@desy.de, melih.oezcelik@kit.edu

ABSTRACT: The energy dependence of the total hadroproduction cross section of pseudo-scalar quarkonia is computed via matching Next-to-Leading Order (NLO) Collinear-Factorisation (CF) results with resummed higher-order corrections, proportional to $\alpha_s^n \ln^{n-1}(1/z)$, to the CF hard-scattering coefficient, where $z = M^2/\hat{s}$ with M and $\hat{s}$ being the quarkonium mass and the partonic center-of-mass energy squared. The resummation is performed using High-Energy Factorisation (HEF) in the Doubly-Logarithmic (DL) approximation, which is a subset of the leading logarithmic $\ln(1/z)$ approximation. Doing so, one remains strictly consistent with the NLO and NNLO DGLAP evolution of the PDFs. By improving the treatment of the small-z asymptotics of the CF coefficient function, the resummation cures the unphysical results of the NLO CF calculation. The matching is directly performed in the z-space and, for the first time, by using the Inverse-Error Weighting (InEW) matching procedure. As a by-product of the calculation, the NNLO term of the CF hard-scattering coefficient proportional to $\alpha_s^2 \ln(1/z)$ is predicted from HEF.

KEYWORDS: Deep Inelastic Scattering or Small-X Physics, Quarkonium, Resummation, Higher-Order Perturbative Calculations

---

[1]Corresponding author.

Contents

1 Introduction: heavy-quarkonium cross-section instability at high energies

Historically, the discovery of charm quarks and charmonia has been one of the most important milestones towards establishing QCD as the theory of strong interaction. Nowadays, charmonia and bottomonia attract a lot of attention as tools to study the proton structure, spin physics and/or to probe the quark-gluon plasma, see e.g. recent reviews [1–5]. They have clean experimental signatures and the fact that the hard scale of their production process is limited from below by the heavy-quark mass justifies the application of perturbation theory. However, the usage of quarkonia as tools for precision studies is problematic because up to now there is no consensus in the community on what are the main mechanisms of quarkonium production. The Non-Relativistic QCD(NRQCD) factorisation approach [6] at NLO in the α_s expansion and NNLO in the v^2 expansion, which seems to be the most systematic theoretical tool available so far, is able to describe the unpolarised p_T-differential hadroproduction cross sections of charmonia [7–13] and bottomonia [14–16]. However, this

approach has essentially failed all other phenomenological tests. It is incapable [7–10] of describing the unpolarised photo- and hadroproduction data together with the data on quarkonium polarisation observables using a single set of Long-Distance Matrix Elements (LDMEs). This problem is known as the "polarisation puzzle". Moreover, the hadroproduction of η_c at the LHC has unexpectedly turned out to be dominated by the color-singlet state $c\bar{c}[^1S_0^{[1]}]$, with no color-octet contribution needed to describe data [17]. This seems inconsistent with heavy-quark spin symmetry relations between the LDMEs of η_c and J/ψ. This inconsistency is often referred to as the "heavy-quark-spin-symmetry puzzle".

Alternative theoretical approaches, such as the (Improved) Colour-Evaporation Model [18–21] have their own phenomenological problems, e.g. being incapable to describe the J/ψ-pair hadroproduction [22], single J/ψ hadroproduction at large p_T [22] or $e^+e^- \to J/\psi + c + \bar{c}$ cross section [3]. Moreover, recent theoretical developments, such as potential-NRQCD [23] or soft-gluon factorisation [24–26] stay within the non-relativistic paradigm for the bound-state and try to either reduce number of free parameters in NRQCD or more accurately treat the kinematic effects of soft gluon emissions at hadronisation stage.

Given the situation described above, the logical way to proceed is to scrutinise all possible sources of numerically large higher-order corrections to the hard-scattering coefficient function in the NRQCD approach beyond fixed-order NLO in α_s computations and find possible ways to resum them to all orders in perturbation theory. For example, at high p_T, much larger than the quarkonium mass M, such a resummation has already being achieved via the fragmentation formalism which has been worked out up to the next-to-leading power in M/p_T [13, 27]. In the present paper, we focus on a class of higher-order QCD corrections, which has been largely ignored so far in the CF heavy-quarkonium-production literature and which become important when the hadronic collision energy, $\sqrt{s}$, is much larger than any other scale of our process, i.e. M or p_T.

For simplicity, we will focus on the case of the inclusive hadroproduction of the $^1S_0^{[1]}$, $^3P_0^{[1]}$ and $^3P_2^{[1]}$ NRQCD Fock states of a heavy-quark pair of mass M. These states can be produced at LO in CF via a $2 \to 1$ process, namely by fusion of two on-shell gluons. The NLO CF corrections to the total hadroproduction cross section at most involves $2 \to 2$ processes and can be computed in a closed form, which has been done long time ago [28, 29]. In CF, the total hadroproduction cross section of a state $m = {}^{2S+1}L_J^{[1,8]}$ in a $h_A + h_B$ hadronic collision at a center-of-mass energy $\sqrt{s}$ can be computed as a convolution:

$$\sigma^{[m],h_A h_B}(\sqrt{s}) = \sum_{i,j=q,\bar{q},g} \int_{z_{\min}}^{1} \frac{dz}{z} \mathcal{L}_{ij}^{h_A h_B}(z,\mu_F)\hat{\sigma}_{ij}^{[m]}(z,\mu_F,\mu_R), \tag{1.1}$$

over the variable $z = M^2/\hat{s}$ which represents the squared fraction of the energy of the partons initiating the hard subprocess used to produce the observed final-state of mass M, with $z_{\min} = M^2/s$. The partonic luminosity for partons $i,j = q,\bar{q},g$, entering eq. (1.1) is:

$$\mathcal{L}_{ij}^{h_A h_B}(z,\mu_F) = \int_{-y_{\max}}^{+y_{\max}} dy \, \tilde{f}_i^{h_A}\left(\frac{M}{\sqrt{sz}}e^y,\mu_F\right) \tilde{f}_j^{h_B}\left(\frac{M}{\sqrt{sz}}e^{-y},\mu_F\right), \tag{1.2}$$

where $y_{\max} = \ln\sqrt{sz}/M$ and[1] $\tilde{f}_i^h(x, \mu_F^2) = x f_i^h(x, \mu_F^2)$ are the collinear "momentum-density" PDFs of the parton i in a hadron h, evaluated at the factorisation scale μ_F. The quantity $\hat{\sigma}_{ij}^{[m]}$ in eq. (1.1) is the hard-scattering coefficient for the corresponding partonic channel ij and state m.

The partonic luminosity is always decreasing when $z \to M^2/s$ corresponding to $y_{\max} \to 0$. However, at $\mu_F \gg 1\,\mathrm{GeV}$ this decrease is more rapid than at $\mu_F \sim 1\,\mathrm{GeV}$, characteristic of quarkonium physics, due to the μ_F-evolution of the x-dependence of the PDFs in eq. (1.2). It turns out that, at high scales, the contribution of small values of z to the integral (1.1) is suppressed by the partonic luminosity. However, at smaller scales $\mu_F \sim M \sim 1\,\mathrm{GeV}$ most of the recent PDFs are relatively flat as functions of x, and the region of small z starts to significantly contribute to the cross section at high energies $\sqrt{s} \gg M$, see the detailed discussion in ref. [30]. For quarkonium-production cross sections at NLO in CF, the effect of the small-z region is dramatic, as it was understood already in refs. [31, 32].

For our forthcoming discussion, let us express the CF coefficient function from eq. (1.1) as follows:

$$\hat{\sigma}_{ij}^{[m]} = \sigma_0^{[m]} \left[A_0^{[m]} \delta(1-z) + C_{ij} \frac{\alpha_s(\mu_R)}{\pi} \left(A_0^{[m]} \ln \frac{M^2}{\mu_F^2} + A_1^{[m]} \right) + \mathcal{O}(z\alpha_s, \alpha_s^2) \right], \quad (1.3)$$

where the first term in square brackets contributes only for the states $Q\bar{Q}[m]$ which can be produced in fusion of two on-shell gluons at $\mathcal{O}(\alpha_s^2)$. For such states, $A_0^{[m]} = 1$. For all the other $Q\bar{Q}[m]$ states, $A_0^{[m]} = 0$ so that $\hat{\sigma}_{ij}^{[m]}$ starts at $\mathcal{O}(\alpha_s^3)$. The second term in the square brackets of the eq. (1.3) is the $z \to 0$ asymptotics of the $\mathcal{O}(\alpha_s^3)$ part of the coefficient function, while all the remaining terms are collected in the term $\mathcal{O}(\alpha_s z, \alpha_s^2)$. The global factors $\sigma_0^{[m]}$ are defined in eq. (2.12) below.

The Fock-state-dependent constants $A_1^{[m]}$ in eq. (1.3) are collected, for the cases when $A_0^{[m]} \neq 0$, in table 1 of ref. [30] and they turn out to be negative. The colour-factors C_{ij} in eq. (1.3) are: $C_{gg} = 2C_A = 2N_c$, $C_{qg} = C_{gq} = C_F = (N_c^2 - 1)/(2N_c)$ and $C_{q\bar{q}} = 0$ (with $N_c = 3$ being the number of colours). If the series (1.3) is truncated at NLO in α_s, then for scale choices satisfying $\mu_F \geq M$, the contribution of the region $z \ll 1$ to the integral (1.1) becomes purely negative and, at sufficiently high energies, it may outweigh the positive NLO contribution from the $z \to 1$ limit and even the LO contribution.

For charmonium production characterised by $M \simeq 3\,\mathrm{GeV}$, this already happens at $\sqrt{s}$ as modest as several hundreds of GeV [30, 32] making NLO calculation completely unpredictive at LHC energies. We find the problem described above very interesting because similar instabilities plague the energy-dependence of rapidity-differential cross sections of J/ψ hadroproduction in NRQCD factorisation at NLO [33] and could also affect the p_T-differential cross section at $p_T \lesssim M \ll \sqrt{s}$.

As it was realised in ref. [30], authored by two of us, these negative cross sections in CF at NLO stem from an *over*subtraction of the collinear divergences inside the renormalised PDFs within the $\overline{\mathrm{MS}}$ scheme. In principle, such a subtraction should be compensated by the

---

[1]In what follows, we will omit h_A and h_B when referring to PDFs.

evolution of the PDFs which progressively become steeper when μ_F increases. However, the coefficients A_1, which are related to the internal structure of the $gg \rightarrow Q\bar{Q}[m]$ form factor, are process-dependent as opposed to the PDF evolution governed by the Dokshitzer-Gribov-Lipatov-Altarelli-Parisi (DGLAP) [34–36] equations. As such, the negative numbers cannot be systematically compensated by the PDF evolution. This mismatch between the partonic cross section and the PDFs is most dramatic for low scale processes for which the PDFs are the flattest.

The small-z behaviour of the NLO partonic cross section of the type (1.3) is characteristic of many hard processes, as it was shown for the first time in ref. [37] for the cases of total open heavy-flavour hadro- and photoproduction as well as prompt-photon hadroproduction. In these cases, the coefficients A_1 turn out to be positive, whereas they are negative for the hadroproduction of $^1S_0$, $^3P_0$ and $^3P_2$-states of heavy quark-anti-quark pairs as mentioned above, as well as for the photoproduction of $^3S_1$ [38]. For Higgs-boson hadroproduction, the sign of the coefficient A_1 depends on the ratio M_{H^0}/m_t (see ref. [30]). These observations clearly point at the fact that it is impossible to absorb the impact of A_1 into the PDFs via the global scheme redefinition proposed in ref. [37]: the optimal subtraction scheme for the open heavy-flavour hadroproduction will be worse than $\overline{\text{MS}}$ for heavy quarkonia at high energies, and vice-versa.

In ref. [30], two of us have proposed a new scale prescription for the factorisation scale to cure the mismatch between the partonic cross section and the PDF evolution (for processes with $A_0 = 1$):

$$\hat{\mu}_F = M \exp\left[A_1^{[m]}/2\right], \tag{1.4}$$

which restores the positivity of quarkonium-production cross sections (see refs. [30, 38]). As it will be explained in section 2.5, this scale choice corresponds to an attempt to resum some higher-order QCD corrections proportional to:

$$\alpha_s^n \ln^{n-1} \frac{1}{z}, \tag{1.5}$$

at leading power in z for $z \ll 1$ within $\hat{\sigma}_{ij}$. In what follows, we will refer to the all order in α_s resummation of the contributions of the type (1.5) as the *Leading Logarithmic-*$\ln(1/z)$ *Approximation* or LL($\ln(1/z)$) for short. The advantage of the $\hat{\mu}_F$-prescription in comparison to the global scheme redefinition is that it is process-dependent, i.e. every process is evaluated with its own scale (1.4).

However, beyond $\mathcal{O}(\alpha_s)$, the approximate resummation via the $\hat{\mu}_F$-prescription does not correctly capture the structure of QCD corrections of the type (1.5). For instance, as we will see, the $\alpha_s^2 \ln 1/z$ coefficient of the expanded expression of the NLO cross section obtained with $\mu_F = \hat{\mu}_F$ does not correspond to the one obtained from the resummation formalism. The systematic formalism for such a resummation requires the use of the Balitsky-Fadin-Kuraev-Lipatov (BFKL) evolution [39–41] of the partonic amplitude in the rapidity $Y \sim \ln(1/z) \gg 1$ with its non-trivial transverse-momentum dynamics to correctly capture higher-order QCD corrections even in the LL($\ln(1/z)$) approximation. Such a formalism is known as *High Energy Factorisation (HEF)* and has been developed in refs. [42–45] in the LL($\ln(1/z)$) approximation. In the past, this formalism has been

successfully applied to study the high-energy structure of hard-scattering coefficients of CF for many processes, such as heavy-flavor leptoproduction [46], Higgs [47, 48], Drell-Yan lepton-pair [49] and prompt-photon production [50]. In particular, in ref. [49] the correctness of the resummation predictions up to NNLO in α_s has been verified. Recently, the NLL($\ln(1/z)$) resummation for lepton-hadron Deep-Inelastic Scattering has been shown to significantly improve the quality of NNLO PDF fits [51, 52].

With the present paper, we fill the gap in the existing HEF literature, providing the first NLO CF + LL($\ln(1/z)$) matched calculation of the energy dependence of the total heavy-quarkonium-hadroproduction cross section. The aforementioned HEF calculations [46–50] use the representation of the resummed cross section in Mellin space, which is convenient from the computational point of view, but is difficult to match with NLO CF results. For example, in the ref. [46] the matching between LL HEF and NLO CF calculations has been implemented via subtractive prescription in the Mellin space (N) conjugate to z. With such a technique, however, it would be quite difficult to come up with any alternative matching prescription, which is necessary to estimate the uncertainty on the obtained cross section results due to matching procedure. In contrast, we perform a direct z-space matching between the HEF-resummed hard-scattering coefficient, which is valid at $z \ll 1$, and the full NLO CF correction, which contains numerically important $\mathcal{O}(z)$ power corrections. Along the same lines of the ref. [53], we propose a new matching procedure, described in section 3.2, which smoothly interpolates between $z \to 0$ and $z \to 1$ limits.

Let us also discuss now the relation of our work with other approaches to quarkonium production at high energies existing in the small-x physics literature, such as calculations of the J/ψ-hadroproduction cross section within Color-Glass-Condensate (CGC) formalism in refs. [54, 55]. In these papers, the all-order-in-α_s resummation of radiative corrections to the *observable cross section* $\sigma(\sqrt{s})$ enhanced by $\ln(s/M^2)$ was the primary objective. The CGC formalism in principle includes all such corrections in the LLA w.r.t. $\ln(s/M^2)$ in the limit $\sqrt{s} \gg M$, yet disregarding[2] the "twist" expansion in powers of the hard scale M^2. In contrast, in the present study, we are resumming large logarithms (1.5) in the coefficient function of the CF $\hat{\sigma}(z)$, i.e. we are working in the leading power approximation w.r.t. the hard scale M^2. As such, our calculation includes at least partially the leading-twist part of the logarithmic corrections resummed in [54, 55]. Indeed, at relatively small scales $\mu_F \sim M \sim 1\,\text{GeV}$, the partonic luminosity function $\mathcal{L}_{ij}(z, \mu_F)$ in eq. (1.1) varies slowly for all values of z except those very close to the kinematic endpoint $z_{\min} = M^2/s$, where it abruptly goes to zero, and therefore large logarithms (1.5) in $\hat{\sigma}$ lead to the contributions proportional to:

$$\int\limits_{z_{\min}}^{1} \frac{dz}{z}\, \alpha_s^n \ln^{n-1} \frac{1}{z} \sim \alpha_s^n \ln^n \frac{1}{z_{\min}} = \alpha_s^n \ln^n \frac{s}{M^2}, \tag{1.6}$$

which is another way to explain why the corrections of the type (1.5) are especially important at $s \gg M^2$. The logarithmic contributions of the type (1.6) can not be

---

[2]It is interesting to note, that the *colour-singlet* $Q\bar{Q}[^3S_1^{(1)}]$ state is produced in refs. [54, 55] via the *subleading twist* contribution, $g + (g + g) \to Q\bar{Q}[^3S_1^{(1)}]$, requiring at least *two* off-shell gluons to be taken from the "target" proton or nucleus. The leading-twist process $g + g \to Q\bar{Q}[^3S_1^{(1)}] + g$ appears at NLO in α_s in the CGC counting.

resummed completely in our calculation, because the HEF formalism is based on the linear BFKL equation, while corrections of the type (1.6) lead to the non-linear effects already in the LLA($\ln(s/M^2)$). These are taken into account, in the planar limit, by Balitsky-Kovchegov [56, 57] or exactly in N_c, by (Balitsky-)Jalilian-Marian-Iancu-McLerran-Weigert-Leonidov-Kovner [58–63] evolution equations. However, we believe that for single-scale observables, such as the total cross section $\sigma(\sqrt{s})$, in the leading twist approximation, all LLA contributions of the type (1.6) can be included into the LLA HEF calculation either via the perturbative resummation of logarithms (1.5) in $\hat{\sigma}$ or phenomenologically, via a modification of the x dependence of the collinear PDFs. This point of view is supported by the fact that higher-twist corrections originating from the modification of the $\mathbf{q}_T$-dependence of the HEF resummation function in the region $|\mathbf{q}_T| \ll M$ are small, see appendix C. Our conclusion is that the resummation of logarithms (1.5) as well as its smooth matching with the NLO CF corrections at $z \sim 1$ are the most numerically important effects for the single-scale observables such as $\sigma(\sqrt{s})$ at high energy and in the leading-twist approximation.

The paper has the following structure. In section 2, we describe the LL($\ln(1/z)$) HEF formalism, in particular the structure of the resummed partonic cross section in z-space (section 2.1), the corresponding process-dependent coefficient functions (section 2.2) and the universal resummation factors (section 2.3). In section 2.4, we expand the resummed cross section up to NNLO in α_s to verify its consistency with NLO results [28, 29] and provide predictions for future NNLO calculations of quarkonium production cross section. In section 2.5, we explain the relation of the HEF formalism with $\hat{\mu}_F$ scale prescription. In section 3, we introduce two matching procedures in z-space, compare the corresponding numerical results and discuss the uncertainties of our calculation. Finally, in section 4, we summarise our conclusions and prospects for future studies. The paper contains three appendices: in appendix A, we explain two methods which we have developed to calculate the resummed cross section in z-space in a numerically-stable way. In appendix B, we show the numerical effects of the $\mathcal{O}(\alpha_s^2)$ corrections to the anomalous dimension (2.20) on the μ_F dependence of the resummed part of the cross section and, in appendix C, we discuss the possible size of non-perturbative effects, due to the intrinsic transverse momentum of gluons in the proton, on the value of the total quarkonium production cross section in our approximation.

2 High-energy factorisation in the leading-logarithmic approximation

2.1 The resummed cross section in z-space

Considering the qg channel as an example, the corrections proportional to $\alpha_s^n \ln^{n-1} 1/z$ to the QCD hard subprocess for the production of the final-state of interest, $Q\bar{Q}[m]$, with a four-momentum p come from processes with at most n additional partons in the final state:

$$g(p_1) + q(p_2) \rightarrow g(k_1) + g(k_2) + \ldots + Q\bar{Q}[m](p) + \ldots + g(k_{n-1}) + q(k_n), \qquad (2.1)$$
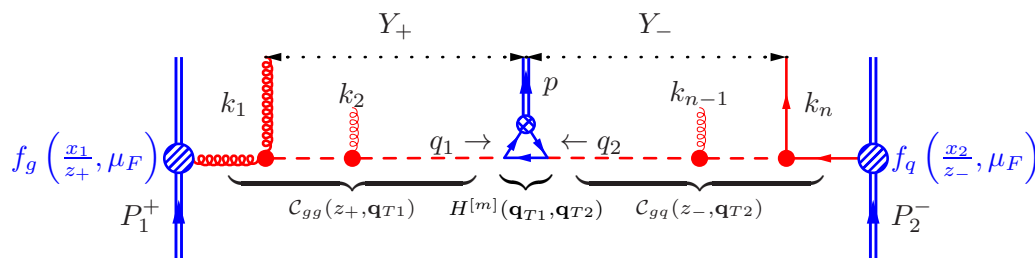
where the four-momentum labels are given in parentheses.

Figure 1. Typical diagrams contributing to the high-energy factorisation amplitude in the gq-channel. The dashed lines denote Reggeised gluon exchanges, while solid circles denote Lipatov's vertices.

At leading-power in z and in the $\mathrm{LL}(\ln(1/z))$ approximation, only the final states with a strong ordering in the corresponding light-cone components of momenta contribute, that is when:

$$p_1^+ \simeq k_1^+ \gg k_2^+ \gg \ldots \gg p^+ \gg \ldots \gg k_{n-1}^+ \gg k_n^+,$$

$$k_1^- \ll k_2^- \ll \ldots \ll p^- \ll \ldots \ll k_{n-1}^- \ll k_n^- \simeq p_2^-,$$

where $k_i^{\pm} = k_i^0 \pm k_i^3$, so that, for the four-momenta of the incoming protons, one has $P_1^+ = \sqrt{s}$, $P_1^- = 0$ and $P_2^+ = 0$, $P_2^- = \sqrt{s}$. This limit is referred to as the *Multi-Regge Kinematics (MRK)*. In this limit and at this accuracy, the QCD amplitudes are known to factorise into a product of gauge-invariant blocks: the Lipatov's scattering, the production vertices [39–41], the t-channel Reggeised gluon propagators and the effective vertex for production of the $Q\bar{Q}[m]$ state, see the figure 1. For a review, the reader can consult the monographs [64, 65] or the lecture notes [66]. This factorisation at the amplitude level allows one to factorise out the corresponding cross-section-level blocks: the universal *resummation factors* $\mathcal{C}_{gi}$, with $i = g, q, \bar{q}$, and the process-dependent *coefficient function* $H^{[m]}$.

The resummation factors are solutions of the BFKL equation, describing the rapidity-evolution of the cascade of emissions from the rapidities of the most backward/forward partons in the hard process to the rapidity of the observed final state. The corresponding rapidity intervals (figure 1) can be estimated in the MRK as:

$$Y_+ = \frac{1}{2}\left(\ln\frac{k_1^+}{k_1^-} - \ln\frac{p^+}{p^-}\right) \simeq \ln\left[\frac{p_1^+}{p_+}\frac{M_T}{|\mathbf{k}_{T1}|}\right] = \ln\frac{1}{z_+} + \ln\frac{M_T}{|\mathbf{k}_{T1}|}, \qquad (2.2)$$

$$Y_- = \frac{1}{2}\left(\ln\frac{p^+}{p^-} - \ln\frac{k_n^+}{k_n^-}\right) \simeq \ln\left[\frac{p_2^-}{p_-}\frac{M_T}{|\mathbf{k}_{Tn}|}\right] = \ln\frac{1}{z_-} + \ln\frac{M_T}{|\mathbf{k}_{Tn}|}, \qquad (2.3)$$

where $M_T^2 = M^2 + \mathbf{p}_T^2$, $z_+ = p_+/p_1^+$ and $z_- = p_-/p_2^-$ are fractions of (+/-) light-cone components entering the hard process, which are used up to produce the final state $Q\bar{Q}[m]$. In terms of z_+ and z_-, the "global" z variable introduced above is equal to:

$$z = \frac{M^2}{\hat{s}} = \frac{M^2}{p_1^+ p_2^-} = \frac{M^2}{M_T^2}z_+ z_-. \qquad (2.4)$$

The LL BFKL evolution of the resummation factors $\mathcal{C}_{gi}$ in rapidity resums higher-order corrections to the cross section proportional to $\alpha_s^n Y_{\pm}^{n-1}$. If one is only interested in

the resummation of the $\ln 1/z$-corrections in the $\mathrm{LL}(\ln(1/z))$ approximation, as we do in the present paper, then one solves the BFKL equation for resummation factors, neglecting transverse-momentum logarithms in eqs. (2.2) and (2.3), i.e. putting $Y_\pm \simeq \ln 1/z_\pm$, as it has been done in the seminal papers [42–45].

If the transverse-momentum logarithms in eqs. (2.2) and (2.3) are not neglected, then in addition to $\ln 1/z$-corrections the HEF actually resums the LL $\alpha_s^n \ln^{2n}(|\mathbf{p}_T|/M)$ and part of the NLL $\alpha_s^n \ln^n(|\mathbf{p}_T|/M)$ corrections, which are traditionally considered within the framework of Transverse-Momentum Dependent (TMD) factorisation [67]. This overlap between TMD and High-Energy factorisations has been explored in recent papers [68, 69].

Postponing a more detailed discussion of the resummation factors until section 2.3, let us write down the factorisation formula for the rapidity-differential cross section in HEF:

$$\frac{d\sigma}{dy} = \sum_{i,j=g,q,\bar{q}} \int\limits_0^\infty d\mathbf{q}_{T1}^2 d\mathbf{q}_{T2}^2 \int\limits_{x_1}^1 \frac{dz_+}{z_+} \tilde{f}_i\left(\frac{x_1}{z_+}, \mu_F\right) \mathcal{C}_{gi}(z_+, \mathbf{q}_{T1}^2, \mu_F, \mu_R)$$

$$\times \int\limits_{x_2}^1 \frac{dz_-}{z_-} \tilde{f}_j\left(\frac{x_2}{z_-}, \mu_F\right) \mathcal{C}_{gj}(z_-, \mathbf{q}_{T2}^2, \mu_F, \mu_R) \int\limits_0^{2\pi} \frac{d\phi}{2} \frac{H^{[m]}(\mathbf{q}_{T1}^2, \mathbf{q}_{T2}^2, \phi)}{M_T^4}, \quad (2.5)$$

where $x_1 = M_T e^y/\sqrt{s}$ and $x_2 = M_T e^{-y}/\sqrt{s}$ with $M_T^2 = M^2 + (\mathbf{q}_{T1} + \mathbf{q}_{T2})^2$ and ϕ being the azimuthal angle between $\mathbf{q}_{T1}$ and $\mathbf{q}_{T2}$. The HEF coefficient function $H^{[m]}$ non-trivially depends on the transverse momenta $\mathbf{q}_{T1,2}$ of the Reggeised gluons entering it (figure 1), and the procedure for its computation is described in section 2.2. As it will become clear below, this transverse-momentum dependence is the key to the factorisation of higher-order terms enhanced by $\ln 1/z$ in the QCD perturbative series in terms of the process-independent resummation functions $\mathcal{C}_{gj}$, encapsulating logarithms $\ln 1/z_\pm$ and the process dependent coefficients $H^{[m]}$, which are free from these large logarithms.

Integrating eq. (2.5) over the rapidity and introducing the variables $\eta = \ln(z_+/z_-)/2$ and z via eq. (2.4), one can recast the total hadronic cross section in HEF into the form of eq. (1.1) with the partonic coefficient:

$$\hat{\sigma}_{ij}^{[m],\,\mathrm{HEF}}(z, \mu_F, \mu_R) = \int\limits_{-\infty}^\infty d\eta \int\limits_0^\infty d\mathbf{q}_{T1}^2 d\mathbf{q}_{T2}^2 \, \mathcal{C}_{gi}\left(\frac{M_T}{M}\sqrt{z}e^\eta, \mathbf{q}_{T1}^2, \mu_F, \mu_R\right)$$

$$\times \mathcal{C}_{gj}\left(\frac{M_T}{M}\sqrt{z}e^{-\eta}, \mathbf{q}_{T2}^2, \mu_F, \mu_R\right) \int\limits_0^{2\pi} \frac{d\phi}{2} \frac{H^{[m]}(\mathbf{q}_{T1}^2, \mathbf{q}_{T2}^2, \phi)}{M_T^4}, \quad (2.6)$$

where the integration over η actually proceeds only over $|\eta| \leq \eta_{\max} = \ln\left[M/(M_T\sqrt{z})\right]$, because the arguments of the resummation functions $z_\pm$ should be smaller or equal to one.

Finally let us emphasise that, for the gg channel, the transverse-momentum integrals in eq. (2.6) can not be dealt with numerically unless the LO contribution $\sigma_0^{[m]}\delta(1-z)$ is explicitly removed from eq. (2.6):

$$\hat{\sigma}_{gg}^{[m],\,\mathrm{HEF}}(z, \mu_F, \mu_R) = \sigma_0^{[m]}\delta(1-z) + \check{\sigma}_{gg}^{[m],\,\mathrm{HEF}}(z, \mu_F, \mu_R), \quad (2.7)$$

where $\check{\sigma}_{gg}^{[m],\,\text{HEF}}$ is the LO-*subtracted* resummed hard-scattering coefficient. The LO CF contribution is contained in the $\hat{\sigma}_{gg}^{[m],\,\text{HEF}}$ because the perturbative expansion for resummation factors $\mathcal{C}_{gg}$ starts with the LO term $\delta(1-z)\delta(\mathbf{q}_T^2)$, which corresponds to the case with no additional emissions. The procedure (2.7) turns the integrals in eq. (2.6) into well-defined functions of z. We describe two methods which we have used to isolate the LO contribution in the appendix A. The method of the section A.1 relies on the form of resummation factor in the Doubly-Logarithmic approximation, which we will introduce in eq. (2.30) in section 2.3, while the method in section A.2 is more general and is applicable to the exact $\text{LL}(\ln(1/z))$ resummation factor (2.18) and its generalisations.

2.2 HEF coefficient functions

For the following $2 \to 1$ processes:

$$R(q_1) + R(q_2) \to c\bar{c}\left[{}^1S_0^{[1,8]},\,{}^3S_1^{[8]},\,{}^3P_{0,1,2}^{[1,8]}\right], \tag{2.8}$$

the corresponding HEF coefficient functions are non-zero at LO in α_s. In eq. (2.8), the incoming Reggeised gluons are denoted by the symbol R and their four-momenta can be parametrised as $q_1^\mu = x_1 P_1^\mu + q_{T1}^\mu$ and $q_2^\mu = x_2 P_2^\mu + q_{T2}^\mu$ (figure 1) so that $q_{1,2}^2 = -\mathbf{q}_{T1,2}^2 < 0$. The Feynman rules of Lipatov's gauge-invariant EFT for Multi-Regge processes in QCD [70] are used for the computation of HEF coefficient functions for general QCD processes, as it was done for quarkonia in ref. [71]. The use of the High-Energy EFT is particularly important for the gauge invariance[3] of the computation of the coefficient function for production of the ${}^3S_1^{[8]}$-state. Essentially, the Lipatov's vertex should be used instead of the usual three-gluon vertex.[4]

In the present paper we take the explicit expressions for HEF coefficient functions, which can be directly plugged into our eq. (2.6), from ref. [75]. The HEF coefficient functions satisfy the on-shell-limit normalisation condition:

$$\int\limits_0^{2\pi} \frac{d\phi}{2\pi} \lim_{\mathbf{q}_{T1,2}^2 \to 0} H^{[m]}(\mathbf{q}_{T1}^2, \mathbf{q}_{T2}^2, \phi) = \frac{1}{4(N_c^2-1)^2} \sum_{\lambda_{1,2}=\pm} \left|\mathcal{M}(g_{\lambda_1}g_{\lambda_2} \to Q\bar{Q}[m])\right|^2, \tag{2.10}$$

with the corresponding CF squared amplitude $\mathcal{M}$ averaged over colours and helicities $\lambda_{1,2}$ of the initial-state gluons. It is convenient to separate out the corresponding colour

---

[3]With respect to gauge choice of internal gluon propagator.

[4]Indeed, for the states listed in eq. (2.8), except for ${}^3S_1^{[8]}$, the EFT computation is equivalent to the use of the following "nonsense" polarisation prescription for the initial-state gluons:

$$\varepsilon^\mu(q_{1,2}) \to \frac{q_{T1,2}^\mu}{|\mathbf{q}_{T1,2}|}, \tag{2.9}$$

due to Slavnov-Taylor identities of QCD. However, for more complicated processes containing final-state gluons coupling to initial-state ones, or otherwise essentially non-Abelian, as e.g. double color-octet channels in heavy-quarkonium pair production [72], the full set of Feynman rules of the EFT [70] have to be used instead of the prescription (2.9). The coefficient functions for the processes (2.8) have been computed for the first time in [73–75] using the prescription (2.9) and later have been reproduced in the ref. [71] using Lipatov's EFT.

factors, the LDMEs of NRQCD $\langle \mathcal{O}[m] \rangle$ and the CF spin-orbital factors from the coefficient functions as follows:

$$H^{[m]}(\mathbf{q}_{T1}^2, \mathbf{q}_{T2}^2, \phi) = \frac{M^4 \sigma_0^{[m]}}{\pi} F^{[m]}(\mathbf{q}_{T1}^2, \mathbf{q}_{T2}^2, \phi), \qquad (2.11)$$

where the $\sigma_0^{[m]}$ factors are:

$$\sigma_0^{[^1S_0^{[1]}]} = \frac{8}{C_A^3 C_F} \pi^3 \alpha_s^2 \frac{\langle \mathcal{O}[^1S_0^{[1]}] \rangle}{M^5}, \qquad (2.12)$$

$$\sigma_0^{[^1S_0^{[8]}]} = \frac{4(C_A^2 - 4)}{C_A^3 C_F^2} \pi^3 \alpha_s^2 \frac{\langle \mathcal{O}[^1S_0^{[8]}] \rangle}{M^5},$$

$$\sigma_0^{[^3S_1^{[8]}]} = \frac{8(C_A - 2C_F)}{3C_F^2} \pi^3 \alpha_s^2 \frac{\langle \mathcal{O}[^3S_1^{[8]}] \rangle}{M^5},$$

$$\sigma_0^{[^3P_0^{[1]}]} = \frac{96}{C_A^3 C_F} \pi^3 \alpha_s^2 \frac{\langle \mathcal{O}[^3P_0^{[1]}] \rangle}{M^7},$$

$$\sigma_0^{[^3P_1^{[1]}]} = \frac{192}{C_A^3 C_F} \pi^3 \alpha_s^2 \frac{\langle \mathcal{O}[^3P_1^{[1]}] \rangle}{M^7},$$

$$\sigma_0^{[^3P_2^{[1]}]} = \frac{128}{5C_A^3 C_F} \pi^3 \alpha_s^2 \frac{\langle \mathcal{O}[^3P_2^{[1]}] \rangle}{M^7},$$

$$\sigma_0^{[^3P_0^{[8]}]} = \frac{48(C_A^2 - 4)}{C_A^3 C_F^2} \pi^3 \alpha_s^2 \frac{\langle \mathcal{O}[^3P_0^{[8]}] \rangle}{M^7},$$

$$\sigma_0^{[^3P_1^{[8]}]} = \frac{96(C_A^2 - 4)}{C_A^3 C_F^2} \pi^3 \alpha_s^2 \frac{\langle \mathcal{O}[^3P_1^{[8]}] \rangle}{M^7},$$

$$\sigma_0^{[^3P_2^{[8]}]} = \frac{64(C_A^2 - 4)}{5C_A^3 C_F^2} \pi^3 \alpha_s^2 \frac{\langle \mathcal{O}[^3P_2^{[8]}] \rangle}{M^7},$$

where $C_A = N_c$, $C_F = (N_c^2 - 1)/(2N_c)$ and the averaging factors accounting for the number of polarisation $(2J + 1)$ and colour-singlet $(2N_c)$ or colour-octet $(N_c^2 - 1)$ states of the $Q\bar{Q}[m]$-pair have been included into the denominators of eqs. (2.12) according to the standard definition of LDMEs. The functions $F^{[m]}$ in the eq. (2.11) do not depend on the colour state of the $Q\bar{Q}$ pair and depend only on its spin and orbital momentum. For the S-states they are:

$$F^{[^1S_0]}(t_1, t_2, \phi) = 2 \frac{(M^2 + \mathbf{p}_T^2)^2}{(M^2 + t_1 + t_2)^2} \sin^2 \phi, \qquad (2.13)$$

$$F^{[^3S_1]}(t_1, t_2, \phi) = \frac{(M^2 + \mathbf{p}_T^2)\left[(t_1 + t_2)^2 + M^2\left(t_1 + t_2 - 2\sqrt{t_1 t_2}\cos\phi\right)\right]}{M^2(M^2 + t_1 + t_2)^2}, \qquad (2.14)$$

with $\mathbf{p}_T^2 = (\mathbf{q}_{T1} + \mathbf{q}_{T2})^2 = t_1 + t_2 + 2\sqrt{t_1 t_2}\cos\phi$ with $t_{1,2} = \mathbf{q}_{T1,2}^2$. For the P-wave states,

one has:

$$F^{[^3P_0]}(t_1, t_2, \phi) = \frac{2}{9} \frac{\left(M^2 + \mathbf{p}_T^2\right)^2 \left[(3M^2 + t_1 + t_2)\cos\phi + 2\sqrt{t_1 t_2}\right]^2}{(M^2 + t_1 + t_2)^4},$$

$$F^{[^3P_1]}(t_1, t_2, \phi) = \frac{2}{9} \frac{\left(M^2 + \mathbf{p}_T^2\right)^2 \left[(t_1 + t_2)^2 \sin^2\phi + M^2\left(t_1 + t_2 - 2\sqrt{t_1 t_2}\cos\phi\right)\right]}{(M^2 + t_1 + t_2)^4},$$

$$F^{[^3P_2]}(t_1, t_2, \phi) = \frac{1}{3} \frac{\left(M^2 + \mathbf{p}_T^2\right)^2}{(M^2 + t_1 + t_2)^4} \left\{ 3M^4 + 3M^2(t_1 + t_2) + 4t_1 t_2 \right. \tag{2.15}$$

$$\left. + (t_1 + t_2)^2 \cos^2\phi + 2\sqrt{t_1 t_2}\left[3M^2 + 2(t_1 + t_2)\right]\cos\phi \right\}.$$

The on-shell limits (2.10) of the functions $F^{[m]}$ are equal to one or zero, depending on whether the corresponding state is allowed to be produced in a fusion of two on-shell gluons by the Landau-Yang theorem, i.e. they are equal to constants A_0 first introduced in eq. (1.3).

2.3 Resummation factor in the doubly-logarithmic approximation and beyond

Following the original refs. [42–45], we introduce the Mellin transform with respect to the z-dependence of the resummation factor as follows:

$$\mathcal{C}(N, \mathbf{q}_T, \mu_F, \mu_R) = \int\limits_0^1 dz \, z^{N-1} \mathcal{C}(z, \mathbf{q}_T, \mu_F, \mu_R), \tag{2.16}$$

so that the logarithms which we aim to resum are mapped to poles at $N = 0$ in Mellin space:

$$\ln^{k-1} \frac{1}{z} \leftrightarrow \frac{(k-1)!}{N^k}. \tag{2.17}$$

The emissions of additional partons at higher orders in α_s generate collinear divergences in the resummation factor which have been removed in ref. [44] using a transverse-momentum cut off and using dimensional regularisation and the $\overline{\text{MS}}$-subtraction prescription in ref. [45]. After the subtraction of the collinear divergences, the dependence on factorisation scale μ_F arises in the resummation factor. The Mellin-space result [42–45] for the subtracted resummation factor is:

$$\mathcal{C}_{gg}(N, \mathbf{q}_T^2, \mu_F, \mu_R) = R(\gamma_{gg}(N, \alpha_s)) \frac{\gamma_{gg}(N, \alpha_s)}{\mathbf{q}_T^2} \left(\frac{\mathbf{q}_T^2}{\mu_F^2}\right)^{\gamma_{gg}(N, \alpha_s)}, \tag{2.18}$$

where $\hat{\alpha}_s = \alpha_s(\mu_R)C_A/\pi$. The choice of the scale at which the α_s is evaluated in the $\mathcal{C}_{gg}$ function is not strictly dictated by the LL(ln(1/z)) resummation or NLO CF results. However, since both $\mathcal{C}_{gg}$ functions and HEF coefficient function belong to coefficient function of CF $\hat{\sigma}_{ij}^{[m]}$ (see eq. (2.6)), we opt to choose the same scale μ_R of the α_s in all these quantities. The anomalous dimension γ_{gg} is the solution of the algebraic equation first derived in the ref. [76]:

$$\frac{\hat{\alpha}_s}{N} \chi(\gamma_{gg}(N, \alpha_s)) = 1, \tag{2.19}$$

where $\chi(\gamma) = 2\psi_0(1) - \psi_0(\gamma) - \psi_0(1 - \gamma)$ is he Lipatov's LO characteristic function and $\psi_n(\gamma) = d^n \ln \Gamma(\gamma)/d\gamma^n$ is the Euler's ψ function. The first few terms of the perturbative solution of eq. (2.19) are:

$$\gamma_{gg}(N, \alpha_s) = \gamma_N + 2\zeta(3)\frac{\hat{\alpha}_s^4(\mu_R)}{N^4} + 2\zeta(5)\frac{\hat{\alpha}_s^6(\mu_R)}{N^6} + \mathcal{O}(\alpha_s^7), \text{ where } \gamma_N = \frac{\hat{\alpha}_s(\mu_R)}{N}. \quad (2.20)$$

Eq. (2.18) and the anomalous dimension (2.20) resum the series of higher-order corrections proportional to α_s^n/N^n. These corrections by virtue of the mapping (2.17) are equivalent to the LL($\ln(1/z)$)-approximation (1.5). While the LL($\ln(1/z)$) anomalous dimension (2.20) is scheme-independent in a wide class of $\overline{\text{MS}}$-like schemes [45], the factor $R(\gamma)$ encapsulates the subtraction-scheme dependence. For the $\overline{\text{MS}}$ scheme, its perturbative expansion starts at N^{3}LO [45, 77]:

$$R(\gamma_{gg}(N, \alpha_s)) = 1 + \mathcal{O}(\alpha_s^3). \quad (2.21)$$

Let us now define the resummation factors for the quark-induced channels. As depicted in figure 1, in the LL($\ln(1/z)$)-approximation, only Reggeised gluons can propagate in the t-channel. Hence, the quarks can only participate in the so-called LO *partonic impact factors*. The corresponding expression for the squared amplitude in the LL($\ln(1/z)$) approximation differs from the similar squared amplitude with gluon substituted by the quark only by an overall colour factor. This picture leads to the simple relation between the quark and gluon-induced resummation factors in the LL($\ln(1/z)$) approximation:

$$\mathcal{C}_{gq}(z, \mathbf{q}_T^2, \mu_F, \mu_R) = \frac{C_F}{C_A}\left[\mathcal{C}_{gg}(z, \mathbf{q}_T^2, \mu_F, \mu_R) - \delta(1 - z)\delta(\mathbf{q}_T^2)\right], \quad (2.22)$$

where the subtraction term in square brackets removes the contribution of the direct $g \to R$ transition in the on-shell limit. The latter is absent in case of quarks due to the fermion-number conservation.

To clarify the physical meaning of the anomalous dimension γ_{gg} in eq. (2.18), let us observe that, since the Mellin transform turns $z_{\pm}$−convolutions in eq. (2.5) into products, the μ_F independence of the cross section order by order in α_s is achieved provided that:

$$\sum_{i=q,\bar{q},g} \frac{\partial}{\partial \ln \mu_F^2}\left[\tilde{f}_i(N, \mu_F)\mathcal{C}_{gi}(N, \mathbf{q}_T^2, \mu_F, \mu_R)\right] = 0, \quad (2.23)$$

at any $\mathbf{q}_T$. Substituting eqs. (2.18) and (2.22) one finds that eq. (2.23) is indeed satisfied due to the following form of DGLAP equations at LL($\ln 1/z$) accuracy:

$$\frac{\partial \tilde{f}_g(N, \mu_F)}{\partial \ln \mu_F^2} = \gamma_{gg}(N, \alpha_s)\left[\tilde{f}_g(N, \mu_F) + \frac{C_F}{C_A}\sum_{i=q,\bar{q}}\tilde{f}_i(N, \mu_F)\right], \quad (2.24)$$

$$\frac{\partial \tilde{f}_q(N, \mu_F)}{\partial \ln \mu_F^2} = 0. \quad (2.25)$$

In other words, the $\gamma_{gg}(N, \alpha_s)$ is the LL($\ln(1/z)$) approximation to the anomalous dimension of the DGLAP equations, governing the scale dependence of the gluon momentum

density distribution, while $C_F \gamma_{gg}/C_A$ determines the feed down from quarks to gluon in this approximation. Indeed, the corresponding LO DGLAP splitting functions have the following $z \to 0$ asymptotics:

$$\frac{\alpha_s}{2\pi} z P_{gg}(z) = \hat{\alpha}_s + \mathcal{O}(z), \tag{2.26}$$

$$\frac{\alpha_s}{2\pi} z P_{gq}(z) = \frac{C_F}{C_A} \hat{\alpha}_s + \mathcal{O}(z). \tag{2.27}$$

Eq. (2.26) is equivalent to the first term of the solution (2.20) via the mapping (2.17), while eq. (2.27) is related in the same way to the first term of the expansion of $C_F \gamma_{gg}/C_A$ in α_s. The coefficients in front of $\alpha_s \ln(1/z)$ and $\alpha_s^2 \ln^2(1/z)$ terms in the NLO and NNLO contributions to $z P_{gg}(z)$ are zero in QCD, consistently with eq. (2.20). The first non-zero contributions at leading power in z beyond LO in α_s in QCD are $\mathcal{O}(\alpha_s^2)$ and $\mathcal{O}(\alpha_s^3 \ln(1/z))$. They belong to the NLL($\ln(1/z)$) approximation and their consistency with NLL($\ln(1/z)$) BFKL predictions has been verified in ref. [78], while the consistency of the LL($\ln(1/z)$) series (2.20) with the DGLAP anomalous dimension in $\mathcal{N} = 4$-supersymmetric Yang-Mills theory in the large-N_c limit has been checked in ref. [79] up to five loops using integrability-based methods.

The connection with the DGLAP anomalous dimension, outlined above, is very important for the phenomenological strategy of the usage of the LL($\ln(1/z)$) resummation. Most of the common PDF sets[5] use the fixed-order approximation for the DGLAP splittings/anomalous dimensions, i.e. no $\ln(1/z)$-resummation is performed in the evolution. In particular, it means that existing LO, NLO and NNLO PDFs contain information only about the γ_N term in the series (2.20). Including further terms of this series into the CF coefficient function via the resummation will only increase the mismatch between the μ_F dependence of PDFs and the resummation factors and, hence, blow up our μ_F-scale uncertainty at high energy.

The goal of the present paper is to use HEF to cure the unphysical behaviour of the CF coefficient function at small z in a way consistent with the NLO DGLAP evolution of PDFs. Therefore, we will use the following *Doubly-Logarithmic approximation (DLA)* for resummation factor, which is obtained by neglecting all terms of the series (2.20) except the first one:

$$\mathcal{C}_{gg}^{\mathrm{DLA}}(N, \mathbf{q}_T, \mu_F, \mu_R) = \frac{\gamma_N}{\mathbf{q}_T^2} \left(\frac{\mathbf{q}_T^2}{\mu_F^2} \right)^{\gamma_N}. \tag{2.28}$$

In the DLA, only terms $\propto \left(\frac{\alpha_s}{N} \ln \frac{\mathbf{q}_T^2}{\mu_F^2} \right)^n \leftrightarrow \alpha_s^n \ln^{n-1} \frac{1}{z} \ln^n \frac{\mathbf{q}_T^2}{\mu_F^2}$ are included in the resummation factor. One also takes $R(\gamma) = 1$ in the eq. (2.28) for the same reason: the corresponding scheme-dependence starts at N³LO, eq. (2.21), and is not taken into account in the NLO or even NNLO PDFs. The inclusion of this factor to the resummation function $\mathcal{C}$ would only lead to an unphysical subtraction-scheme mismatch between the PDFs and the CF coefficient function.

---

[5]With the notable exception of the sets obtained in refs. [51, 52].

The inverse Mellin transform:

$$\mathcal{C}(z, \mathbf{q}_T^2, \mu_F, \mu_R) = \int\limits_{-i\infty}^{+i\infty} \frac{dN}{2\pi i} z^{-N} \mathcal{C}(N, \mathbf{q}_T^2, \mu_F, \mu_R), \qquad (2.29)$$

of the resummation factor in the DLA can be computed straightforwardly, e.g. order-by-order in α_s with the use of relation (2.17), leading to the following result:

$$\mathcal{C}_{gg}^{\mathrm{DLA}}(z, \mathbf{q}_T^2, \mu_F, \mu_R) = \frac{\hat{\alpha}_s(\mu_R)}{\mathbf{q}_T^2} \begin{cases} J_0\left(2\sqrt{\hat{\alpha}_s(\mu_R)\ln\left(\frac{1}{z}\right)\ln\left(\frac{\mu_F^2}{\mathbf{q}_T^2}\right)}\right) & \text{if } \mathbf{q}_T^2 < \mu_F^2, \\[3mm] I_0\left(2\sqrt{\hat{\alpha}_s(\mu_R)\ln\left(\frac{1}{z}\right)\ln\left(\frac{\mathbf{q}_T^2}{\mu_F^2}\right)}\right) & \text{if } \mathbf{q}_T^2 > \mu_F^2, \end{cases} \qquad (2.30)$$

where J_0/I_0 are Bessel functions of first/second kind. Eq. (2.30) is known in the HEF community[6] as the *(Collins-Ellis-)Blümlein formula,* and first appears in ref. [81] where the solution of the evolution equation written in ref. [44] has been studied.

The DLA resummation function (2.28), or equivalently (2.30), has a very important normalisation property:

$$\int\limits_0^{\mu_F^2} d\mathbf{q}_T^2 \, \mathcal{C}_{gg}^{\mathrm{DLA}}(N, \mathbf{q}_T^2, \mu_F, \mu_R) = 1 \leftrightarrow \int\limits_0^{\mu_F^2} d\mathbf{q}_T^2 \, \mathcal{C}_{gg}^{\mathrm{DLA}}(z, \mathbf{q}_T^2, \mu_F, \mu_R) = \delta(1-z), \qquad (2.31)$$

which will be used extensively in the rest of the paper. The similar normalisation condition for $\mathcal{C}_{gq}$ in the DLA follows form eq. (2.22):

$$\int\limits_0^{\mu_F^2} d\mathbf{q}_T^2 \, \mathcal{C}_{gq}^{\mathrm{DLA}}(z, \mathbf{q}_T^2, \mu_F, \mu_R) = 0. \qquad (2.32)$$

2.4 Small-z hard-scattering coefficient at NLO and NNLO from resummation

As a consistency check, the $\mathrm{LL}(\ln(1/z))$ resummation described above should reproduce the small-z behaviour (1.3) of the known NLO result for the coefficient function [28–30]. To this end, one has to expand the resummed CF coefficient functions (2.6) at least up to NLO in α_s. In this section, we perform such an expansion up to NNLO in order to provide predictions for the $\alpha_s^2 \ln(1/z)$ NNLO terms in the CF coefficient functions. The results of this section will also be employed in section 3.2 to construct the weight functions needed for our matching procedure. The DLA resummation factor (2.28) is appropriate for the expansion up to NNLO because the exact $\mathrm{LL}(\ln(1/z))$-resummation factor (2.18) differs from it only starting at $\mathcal{O}(\alpha_s^3)$.

To perform such an expansion, it is convenient to work in Mellin space, plugging in the inverse Mellin transform (2.29) of eqs. (2.28) into eq. (2.6). Passing to the dimensionless transverse momenta $\mathbf{n}_{T1} = \mathbf{q}_{T1}/M$ and $\mathbf{n}_{T2} = \mathbf{q}_{T2}/M$, one can rewrite the resummed CF

---

[6]See e.g. ref. [80] for its application to the inclusive jet production at the LHC.

coefficient functions as:

$$\hat{\sigma}_{ij}^{[m],\,\text{HEF}} = \sigma_0^{[m]} \int\limits_{-\infty}^{\infty} d\eta \int\limits_{-i\infty}^{+i\infty} \frac{dN_+ dN_-}{(2\pi i)^2}\; z^{-\frac{N_+ + N_-}{2}} e^{\eta(N_+ - N_-)} G_{ij}^{[m]}\left(\gamma_{N_+}, \gamma_{N_-}, \frac{N_+ + N_-}{2}, \frac{M^2}{\mu_F^2}\right),$$

(2.33)

where

$$G_{gg}^{[m]}\left(\gamma_1, \gamma_2, \nu, \frac{M^2}{\mu_F^2}\right) = \left(\frac{M^2}{\mu_F^2}\right)^{\gamma_1 + \gamma_2} \int\limits_0^{\infty} \frac{\gamma_1 \gamma_2 d\mathbf{n}_{T1}^2 d\mathbf{n}_{T2}^2}{(\mathbf{n}_{T1}^2)^{1-\gamma_1}(\mathbf{n}_{T2}^2)^{1-\gamma_2}} \int\limits_0^{2\pi} \frac{d\phi}{2\pi} f^{[m]}(\mathbf{n}_{T1}^2, \mathbf{n}_{T2}^2, \phi, \nu),$$

(2.34)

for the gluon channel, while for quark-induced channels, one takes into account eq. (2.22) to obtain

$$G_{qg}^{[m]} = \left(\frac{M^2}{\mu_F^2}\right)^{\gamma_2} \frac{C_F}{C_A} \int\limits_0^{\infty} \frac{\gamma_2 d\mathbf{n}_{T2}^2}{(\mathbf{n}_{T2}^2)^{1-\gamma_2}} \int\limits_0^{\infty} d\mathbf{n}_{T1}^2 \left[\left(\frac{M^2}{\mu_F^2}\right)^{\gamma_1} \gamma_1 (\mathbf{n}_{T1}^2)^{-1+\gamma_1} - \delta(\mathbf{n}_{T1}^2)\right]$$
$$\times \int\limits_0^{2\pi} \frac{d\phi}{2\pi} f^{[m]}(\mathbf{n}_{T1}^2, \mathbf{n}_{T2}^2, \phi),$$

(2.35)

and

$$G_{q\bar{q}}^{[m]} = \left(\frac{C_F}{C_A}\right)^2 \int\limits_0^{\infty} d\mathbf{n}_{T1}^2 d\mathbf{n}_{T2}^2 \left[\left(\frac{M^2}{\mu_F^2}\right)^{\gamma_1} \gamma_1 (\mathbf{n}_{T1}^2)^{-1+\gamma_1} - \delta(\mathbf{n}_{T1}^2)\right]$$
$$\times \left[\left(\frac{M^2}{\mu_F^2}\right)^{\gamma_2} \gamma_2 (\mathbf{n}_{T2}^2)^{-1+\gamma_2} - \delta(\mathbf{n}_{T2}^2)\right] \int\limits_0^{2\pi} \frac{d\phi}{2\pi} f^{[m]}(\mathbf{n}_{T1}^2, \mathbf{n}_{T2}^2, \phi),$$

(2.36)

where, in eqs. (2.34), (2.35) and (2.36), the dimensionless function

$$f^{[m]}(\mathbf{n}_{T1}^2, \mathbf{n}_{T2}^2, \phi, \nu) = \frac{\pi H^{[m]}(M^2 \mathbf{n}_{T1}^2, M^2 \mathbf{n}_{T2}^2, \phi)}{\sigma_0^{[m]} M^4 (1 + (\mathbf{n}_{T1} + \mathbf{n}_{T2})^2)^{2+\nu}} = \frac{F^{[m]}(M^2 \mathbf{n}_{T1}^2, M^2 \mathbf{n}_{T2}^2, \phi)}{(1 + (\mathbf{n}_{T1} + \mathbf{n}_{T2})^2)^{2+\nu}}, \quad (2.37)$$

encapsulates the HEF coefficient function $H^{[m]}$ (or $F^{[m]}$ of eq. (2.11)) and the kinematic factor $1/M_T^4$ from eq. (2.6).

The only quantity depending on α_s in eq. (2.33) is $\gamma_N = \hat{\alpha}_s/N$. One thus only has to Taylor-expand the function $G_{ij}^{[m]}$ with respect to its arguments γ_{N_+} and γ_{N_-}. The corresponding poles in N_+ and N_- map to the following functions of z via eq. (2.33):

$$1 \to \delta(1-z),$$
$$\frac{1}{N_+} \text{ and } \frac{1}{N_-} \to \theta(1-z),$$
$$\frac{1}{N_+^2},\; \frac{1}{N_-^2}, \text{ and } \frac{1}{N_+ N_-} \to \theta(1-z)\ln\frac{1}{z}. \quad (2.38)$$

The expansion of the $\mathbf{n}_{T1,2}^2$ integrand of the function $G_{ij}^{[m]}$ in γ_1 and γ_2 however has to be done in a distributional sense because otherwise the order-by-order integrals will

just diverge at $\mathbf{n}_{T1,2}^2 \to 0$. To this end, one isolates the $\mathbf{n}_{T1,2}^2 \to 0$ behaviour of the $f^{[m]}$ function[7] in the integrands of eqs. (2.34), (2.35) and (2.36) as follows:

$$
\begin{aligned}
f^{[m]}(\mathbf{n}_{T1}^2, \mathbf{n}_{T2}^2, \phi, \nu) = &\Big\{ f^{[m]}(\mathbf{n}_{T1}^2, \mathbf{n}_{T2}^2, \phi, \nu) - f^{[m]}(0, \mathbf{n}_{T2}^2, \phi, \nu)\theta(1 - \mathbf{n}_{T1}^2) \\
&- f^{[m]}(\mathbf{n}_{T1}^2, 0, \phi, \nu)\theta(1 - \mathbf{n}_{T2}^2) + f^{[m]}(0, 0, \phi, \nu)\theta(1 - \mathbf{n}_{T1}^2)\theta(1 - \mathbf{n}_{T2}^2) \Big\} \\
&+ \Big[f^{[m]}(\mathbf{n}_{T1}^2, 0, \phi, \nu) - f^{[m]}(0, 0, \phi, \nu)\theta(1 - \mathbf{n}_{T1}^2) \Big] \theta(1 - \mathbf{n}_{T2}^2) \\
&+ \Big[f^{[m]}(0, \mathbf{n}_{T2}^2, \phi, \nu) - f^{[m]}(0, 0, \phi, \nu)\theta(1 - \mathbf{n}_{T2}^2) \Big] \theta(1 - \mathbf{n}_{T1}^2) \\
&+ f^{[m]}(0, 0, \phi, \nu)\theta(1 - \mathbf{n}_{T1}^2)\theta(1 - \mathbf{n}_{T2}^2).
\end{aligned}
\tag{2.39}
$$

The expression in curly brackets in eq. (2.39) tends to zero when $\mathbf{n}_{T1}^2 \to 0$ and/or $\mathbf{n}_{T2}^2 \to 0$, so the factors $(\mathbf{n}_{T1}^2)^{-1+\gamma_1}$ and $(\mathbf{n}_{T2}^2)^{-1+\gamma_2}$ in front of it in eqs. (2.34)–(2.36) can be safely Taylor-expanded in $\gamma_{1,2}$. The expression in the fourth line of eq. (2.39) tends to zero when $\mathbf{n}_{T1}^2 \to 0$ while its dependence on $\mathbf{n}_{T2}^2$ is just a step function. As a consequence, when this expression is substituted to eqs. (2.34)–(2.36), the dependence on $\mathbf{n}_{T2}^2$ can be integrated out, while the factor $(\mathbf{n}_{T1}^2)^{-1+\gamma_1}$ can be Taylor-expanded in γ_1. For the term in the fifth line of eq. (2.39), the situation is symmetric, up to the replacement $\mathbf{n}_{T1} \leftrightarrow \mathbf{n}_{T2}$. Finally, with the last term in eq. (2.39), the integrations over $\mathbf{n}_{T1}^2$ and $\mathbf{n}_{T2}^2$ can be performed straightforwardly. The resulting expansions for the functions $G_{ij}^{[m]}$ in γ_1 and γ_2 at $\nu = 0$ are:

$$
G_{gg}^{[m]} = \left(\frac{M^2}{\mu_F^2}\right)^{\gamma_1 + \gamma_2} \left[A_0^{[m]} + (\gamma_1 + \gamma_2)A_1^{[m]} + (\gamma_1^2 + \gamma_2^2)A_2^{[m]} + \gamma_1\gamma_2 B_2^{[m]} + \mathcal{O}(\gamma^3) \right].
\tag{2.40}
$$

$$
\begin{aligned}
G_{qg}^{[m]} = \frac{C_F}{C_A}\left(\frac{M^2}{\mu_F^2}\right)^{\gamma_2} &\left\{ \left[\left(\frac{M^2}{\mu_F^2}\right)^{\gamma_1} - 1 \right] A_0^{[m]} + \left(\frac{M^2}{\mu_F^2}\right)^{\gamma_1} (\gamma_1 A_1^{[m]} + \gamma_1^2 A_2^{[m]}) \right. \\
&\left. + \left[\left(\frac{M^2}{\mu_F^2}\right)^{\gamma_1} - 1 \right] (\gamma_2 A_1^{[m]} + \gamma_2^2 A_2^{[m]}) + \left(\frac{M^2}{\mu_F^2}\right)^{\gamma_1} \gamma_1\gamma_2 B_2^{[m]} + \mathcal{O}(\gamma^3) \right\},
\end{aligned}
\tag{2.41}
$$

$$
\begin{aligned}
G_{q\bar{q}}^{[m]} = \left(\frac{C_F}{C_A}\right)^2 &\left\{ \left[\left(\frac{M^2}{\mu_F^2}\right)^{\gamma_1} - 1 \right]\left[\left(\frac{M^2}{\mu_F^2}\right)^{\gamma_2} - 1 \right] A_0^{[m]} \right. \\
&+ \left[\left(\frac{M^2}{\mu_F^2}\right)^{\gamma_2} - 1 \right]\left(\frac{M^2}{\mu_F^2}\right)^{\gamma_1} (\gamma_1 A_1^{[m]} + \gamma_1^2 A_2^{[m]}) \\
&\left. + \left[\left(\frac{M^2}{\mu_F^2}\right)^{\gamma_1} - 1 \right]\left(\frac{M^2}{\mu_F^2}\right)^{\gamma_2} (\gamma_2 A_1^{[m]} + \gamma_2^2 A_2^{[m]}) + \left(\frac{M^2}{\mu_F^2}\right)^{\gamma_1 + \gamma_2} \gamma_1\gamma_2 B_2^{[m]} + \mathcal{O}(\gamma^3) \right\},
\end{aligned}
\tag{2.42}
$$

where the Taylor expansion of the factors $(M^2/\mu_F^2)^{\gamma_{1,2}}$ up to the second order has to be

---

[7]Which can be understood as a test function, on which functionals (2.34), (2.35) and (2.36) depend.

State	$A_0^{[m]}$	$A_1^{[m]}$	$A_2^{[m]}$	$B_2^{[m]}$
$^1S_0$	1	$\mathbf{-1}$	$\frac{\pi^2}{6}$	$\frac{\pi^2}{6}$
$^3S_1$	0	1	0	$\frac{\pi^2}{6}$
$^3P_0$	1	$-\frac{\mathbf{43}}{\mathbf{27}}$	$\frac{\pi^2}{6}+\frac{2}{3}$	$\frac{\pi^2}{6}+\frac{40}{27}$
$^3P_1$	0	$\frac{5}{54}$	$-\frac{1}{9}$	$-\frac{2}{9}$
$^3P_2$	1	$-\frac{\mathbf{53}}{\mathbf{36}}$	$\frac{\pi^2}{6}+\frac{1}{2}$	$\frac{\pi^2}{6}+\frac{11}{9}$

Table 1. Coefficients entering eqs. (2.47)–(2.49) for several states $m = {}^{2S+1}L_J$ of a $Q\bar{Q}$ pair. The highlighted numbers coincide with the corresponding results from the table 1 in ref. [30].

done as well. The coefficients $A_{0,1,2}^{[m]}$ entering this expansion are:

$$A_0^{[m]} = \int\limits_0^{2\pi} \frac{d\phi}{2\pi} f^{[m]}(0,0,\phi,0), \tag{2.43}$$

$$A_1^{[m]} = \int\limits_0^\infty \frac{d\mathbf{n}_{T1}^2}{\mathbf{n}_{T1}^2} \int\limits_0^{2\pi} \frac{d\phi}{2\pi} \left[f^{[m]}(\mathbf{n}_{T1}^2,0,\phi,0) - f^{[m]}(0,0,\phi,0)\theta(1-\mathbf{n}_{T1}^2) \right], \tag{2.44}$$

$$A_2^{[m]} = \int\limits_0^\infty \frac{d\mathbf{n}_{T1}^2}{\mathbf{n}_{T1}^2} \ln \mathbf{n}_{T1}^2 \int\limits_0^{2\pi} \frac{d\phi}{2\pi} \left[f^{[m]}(\mathbf{n}_{T1}^2,0,\phi,0) - f^{[m]}(0,0,\phi,0)\theta(1-\mathbf{n}_{T1}^2) \right], \tag{2.45}$$

while, for the coefficient $B_2^{[m]}$, one has

$$\begin{aligned} B_2^{[m]} = \int\limits_0^\infty \frac{d\mathbf{n}_{T1}^2 d\mathbf{n}_{T2}^2}{\mathbf{n}_{T1}^2 \mathbf{n}_{T2}^2} \int\limits_0^{2\pi} \frac{d\phi}{2\pi} &\left\{ f^{[m]}(\mathbf{n}_{T1}^2,\mathbf{n}_{T2}^2,\phi,0) - f^{[m]}(0,\mathbf{n}_{T2}^2,\phi,0)\theta(1-\mathbf{n}_{T1}^2) \right. \\ &\left. - f^{[m]}(\mathbf{n}_{T1}^2,0,\phi,0)\theta(1-\mathbf{n}_{T2}^2) + f^{[m]}(0,0,\phi,0)\theta(1-\mathbf{n}_{T1}^2)\theta(1-\mathbf{n}_{T2}^2) \right\}. \end{aligned} \tag{2.46}$$

Substituting the expansion (2.40) to eq. (2.33) due to the mappings (2.38), one obtains the following result for the z-dependent CF coefficient function in gg channel:

$$\begin{aligned} \hat{\sigma}_{gg}^{[m],\,\text{HEF}} = \sigma_0^{[m]} &\left\{ A_0^{[m]}\delta(1-z) + \frac{\alpha_s}{\pi} 2C_A \left[A_1^{[m]} + A_0^{[m]} \ln \frac{M^2}{\mu_F^2} \right] \right. \\ &\left. + \left(\frac{\alpha_s}{\pi}\right)^2 C_A^2 \ln\frac{1}{z} \left[2A_2^{[m]} + B_2^{[m]} + 4A_1^{[m]}\ln\frac{M^2}{\mu_F^2} + 2A_0^{[m]}\ln^2\frac{M^2}{\mu_F^2} \right] + \mathcal{O}(\alpha_s^3) \right\}, \end{aligned} \tag{2.47}$$

where $\sigma_0^{[m]}$ has been defined in eq. (2.12). The coefficients $A_{0,1,2}^{[m]}$ and $B_2^{[m]}$ can be computed for various spin-orbital states $m = {}^{2S+1}L_J$ by substituting the HEF coefficient functions from eq. (2.15) to eqs. (2.43), (2.44), (2.45) and (2.46). The results of this computation are listed in the table 1.
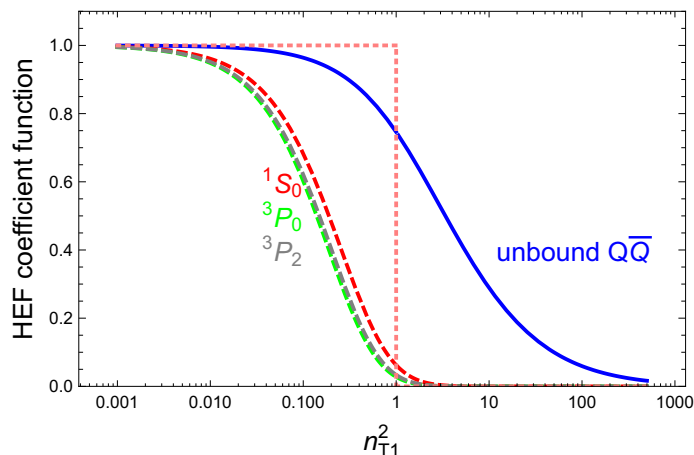
Figure 2. Dimensionless integrand function (2.37) averaged over ϕ, at $\mathbf{n}_{T2}^2 = 0$, as a function of $\mathbf{n}_{T1}^2 = \mathbf{q}_{T1}^2/(4m_Q^2)$, normalised on its value at $\mathbf{n}_{T1}^2 = 0$. The three dashed curves correspond to the coefficient functions for production of $Q\bar{Q}[m]$-states with $m = {}^1S_0$, ${}^3P_0$ and ${}^3P_2$ (section 2.2). The solid curve depicts the coefficient function for the unbound $Q\bar{Q}$-pair production [37], integrated over the phase space of the $Q\bar{Q}$ pair. The short-dashed line represents the $\overline{\text{MS}}$ subtraction term $\theta(1 - \mathbf{n}_{T1}^2)$.

Similarly, from the expansions (2.41) and (2.42), one obtains the following predictions for the small-z behaviour of the quark-induced channels at NLO and NNLO:

$$\hat{\sigma}_{qg}^{[m], \text{ HEF}} = \sigma_0^{[m]} \left\{ \frac{\alpha_s}{\pi} C_F \left[A_1^{[m]} + A_0^{[m]} \ln \frac{M^2}{\mu_F^2} \right] + \left(\frac{\alpha_s}{\pi} \right)^2 C_A C_F \ln \frac{1}{z} \right.$$
$$\left. \times \left[A_2^{[m]} + B_2^{[m]} + 3 A_1^{[m]} \ln \frac{M^2}{\mu_F^2} + \frac{3}{2} A_0^{[m]} \ln^2 \frac{M^2}{\mu_F^2} \right] \right\}, \qquad (2.48)$$

$$\hat{\sigma}_{q\bar{q}}^{[m], \text{ HEF}} = \sigma_0^{[m]} \left(\frac{\alpha_s}{\pi} \right)^2 C_F^2 \ln \frac{1}{z} \left[B_2^{[m]} + 2 A_1^{[m]} \ln \frac{M^2}{\mu_F^2} + A_0^{[m]} \ln^2 \frac{M^2}{\mu_F^2} \right]. \qquad (2.49)$$

Where the same coefficients $A_{0,1,2}^{[m]}$ and $B_2^{[m]}$ appear as in the gg case. The NLO parts of eqs. (2.47) and (2.48) coincide with the $z \to 0$ asymptotics of the full NLO results, obtained in refs. [30, 32], which is yet another non-trivial cross-check of the HEF formalism.

Let us emphasise that the specific transverse-momentum dependence of the HEF coefficient functions is crucial for the consistency of the HEF results with the high-energy limit of the QCD scattering amplitudes. This is very different from the case of TMD factorisation, which is applicable only at $\mathbf{p}_T^2 \ll M^2$. The NLO coefficient $A_1^{[m]}$ is determined by the behaviour of the coefficient function for $\mathbf{p}_T^2 \simeq \mathbf{q}_{T1,2}^2 \sim M^2$ as follows. In the integrand of eq. (2.44), the step-function $\theta(1 - \mathbf{n}_{T1}^2)$ is subtracted from the dimensionless function $f^{[m]}(\mathbf{n}_{T1}^2, 0, \phi, 0)$, which describes the coefficient function in the case when one gluon is off-shell with momenta $\mathbf{q}_{T,1}$ and the second one is on-shell $\mathbf{q}_{T,2}^2 = 0$. In the case of quarkonia, the latter function starts to decrease already for $\mathbf{n}_{T1}^2 = \mathbf{q}_{T1}^2/M^2 < 1$, so the subtraction leads to a large negative contribution, as illustrated by the plot in the figure 2. For comparison, the coefficient function for open heavy flavour production, integrated over

– 18 –

the phase-space of the final-state heavy quarks, given by eqs. (4.8)–(4.10) in ref. [37], is also plotted in figure 2. From this figure, one immediately realises that the bound state is easily broken by the transverse-momentum imbalance between the incoming off-shell gluons, which leads to a quickly decreasing HEF coefficient function. This dependence is quite different from the "expectation" of the $\overline{\text{MS}}$ scheme,[8] according to which the coefficient function should behave roughly like $\theta(1 - \mathbf{q}_{T1,2}^2/M^2)$ thus leading to the consequent over-subtraction of the collinear behaviour. For the case of open heavy flavour, integrated over its invariant mass, the situation is opposite and the coefficient function has a substantial tail at $\mathbf{q}_{T1,2}^2 > M^2$, which leads to large positive NLO corrections at high energy.

2.5 Resummation by a μ_F choice

The connection between the HEF resummation and the μ_F-scale optimisation approach (the $\hat{\mu}_F$ prescription) proposed in ref. [30] is most easily illustrated by eq. (2.34). Substituting the scale choice (1.4), one obtains:

$$G_{gg}^{[m]}\left(\gamma_{N_+}, \gamma_{N_-}, \nu, \frac{M^2}{\hat{\mu}_F^2}\right) = \exp\left[-A_1^{[m]}(\gamma_{N_+} + \gamma_{N_-})\right] \tag{2.50}$$

$$\times \int\limits_0^\infty \frac{\gamma_{N_+}\gamma_{N_-} d\mathbf{n}_{T1}^2 d\mathbf{n}_{T2}^2}{(\mathbf{n}_{T1}^2)^{1-\gamma_{N_+}}(\mathbf{n}_{T2}^2)^{1-\gamma_{N_-}}} \int\limits_0^{2\pi} \frac{d\phi}{2\pi} f^{[m]}(\mathbf{n}_{T1}^2, \mathbf{n}_{T2}^2, \phi, \nu).$$

The exponent in the first line of eq. (2.50), which arose from the scale choice (1.4), resums a series of corrections proportional to $\gamma_{N_\pm}^n = \hat{\alpha}_s^n/N_\pm^n$, which belong to the LL(ln(1/z))-approximation. This resummation would be equivalent to that performed by the HEF only if this exponent is able to cancel the $\gamma_{N_\pm}$ dependence of the integral in the second line of eq. (2.50). If this was the case then all LL(ln(1/z)) corrections would be removed from the CF coefficient function and absorbed into the scale evolution of PDFs. However, such a perfect cancellation is possible only if the dimensionless function $f^{[m]}$ complies to the relation:

$$\int\limits_0^{2\pi} \frac{d\phi}{2\pi} f^{[m]}(\mathbf{n}_{T1}^2, \mathbf{n}_{T2}^2, \phi, \nu) = \theta\left(e^{A_1^{[m]}} - \mathbf{n}_{T1}^2\right)\theta\left(e^{A_1^{[m]}} - \mathbf{n}_{T2}^2\right), \tag{2.51}$$

which when substituted to the eq. (2.50) leads to $G_{gg}^{[m]}\left(\gamma_{N_+}, \gamma_{N_-}, \nu, M^2/\hat{\mu}_F^2\right) = 1$. Neither the coefficient functions for quarkonium production listed in the section 2.2, nor any other coefficient functions for physical processes known to the authors provide a sharp cut-off in the transverse momentum as in eq. (2.51). Instead, they always smoothly depend on transverse momenta, as e.g. in the figure 2. Therefore, the HEF is not equivalent to the $\hat{\mu}_F$ prescription. By construction, the $\hat{\mu}_F$ prescription takes into account the coefficient $A_1^{[m]}$ and, hence, it is correct up to NLO in α_s. However, already at NNLO in α_s, the results of HEF and the $\hat{\mu}_F$ prescription differ. This is clear because the NNLO coefficients obtained from HEF (table 1) contain the transcendental number $\pi^2/6$, which can not arise from the expansion of the exponent in the first line of eq. (2.50).

---

[8]See e.g. section 3.4 of ref. [67] for the relation of the $\overline{\text{MS}}$ subtraction of $1/\epsilon$ singularity with the transverse momentum cut off.
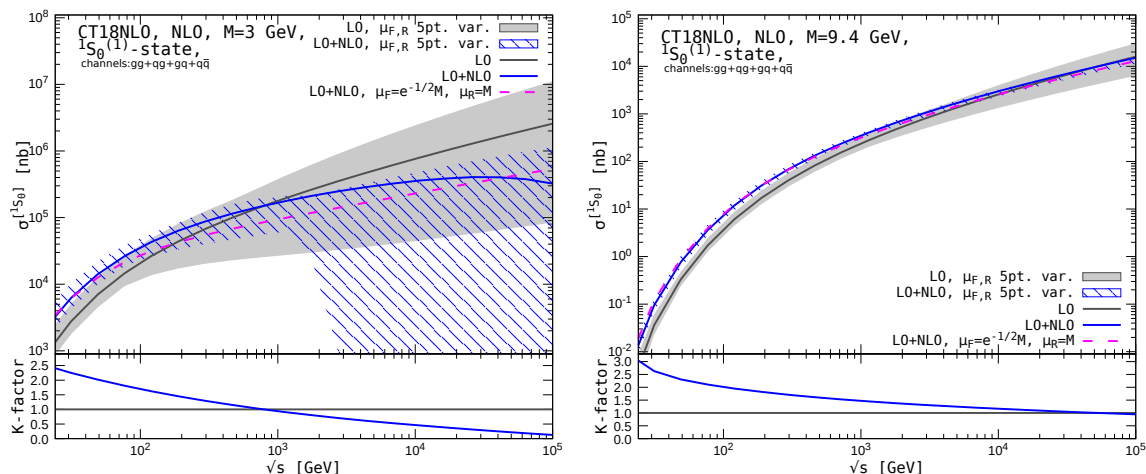
Figure 3. Comparison of the energy dependence of the hadroproduction cross sections of a $Q\bar{Q}[^1S_0^{(1)}]$ state with $M = 3\,\mathrm{GeV}$ (*left panel*) and $M = 9.4\,\mathrm{GeV}$ (*right panel*) in CF at LO (grey curve) and NLO(blue curve). The central member of the CT18NLO PDF set [82] has been used. The dashed line depicts the central prediction of the NLO calculation using the $\hat{\mu}_F$ prescription (equation (1.4)) [30]. The LDME $\langle\mathcal{O}[^1S_0^{(1)}]\rangle$ was set to $1\,\mathrm{GeV}^3$ in both cases for illustration purposes.

3 NLO+DLA matching in z-space

Before discussing various approaches to match the DLA HEF and NLO CF contributions into a single prediction for the total cross section, let us set the baseline by showing how the NLO CF cross section with the "canonical" scale choice $\mu_F = \mu_R = M$ depends on the energy and how large the associated scale uncertainty is. The plots of figure 3 show the LO and NLO CF predictions for the total cross section of the production of $^1S_0^{[1]}$ states with masses of 3 and 9.4 GeV. The scale uncertainties, depicted as solid or shaded bands in all these plots, has been estimated using the five-point scale-variation procedure. The latter procedure consists in evaluating the cross section for each value of the energy with the scale choice $\mu_F = 2^{\zeta_1}M$ and $\mu_R = 2^{\zeta_2}M$ for $(\zeta_1, \zeta_2) \in \{(0, \pm 1), (\pm 1, 0)\}$ and taking, as an uncertainty estimate, the largest positive or negative deviation of the obtained value form the cross section with the default scale choice.

From the left panel of figure 3, one can see that, for $c\bar{c}$ states, the instability of the cross section at high energy is dramatic. Above $\sqrt{s} = 1\,\mathrm{TeV}$, such a computation does not show any more predictive power and, above $\sqrt{s} = 100\,\mathrm{GeV}$, the NLO K factor, defined as the ratio of the NLO to the LO cross section, decreases with energy, which is very different from the behaviour of the matched result as we will see. For bottomonia (see the plot in the right panel of figure 3), the situation is much better: the scale uncertainty of the NLO calculation is significantly smaller than the LO one all the way up to $\sqrt{s} \sim 100\,\mathrm{TeV}$. However, the decrease of the NLO K factor is evident even at this scales. The dependence of this behaviour on the PDF choice has been analysed in detail in ref. [30].

A specific factorisation scale choice (1.4) has been proposed in ref. [30] as a possible resolution of the problem of high-energy instability of quarkonium hadroproduction cross sections. As we have shown in section 2.5, this prescription is equivalent to the resummation

of some LL($\ln 1/z$)-terms, which is correct at NLO but fails at higher orders. In practice, for η_Q hadroproduction, this procedure leads to significantly smaller cross section at high energies, shown by dashed lines in figure 3, than that predicted by LO CF at the default scale. Indeed the PDFs are less evolved thus smaller. In this regards, we stress that, for other processes like H^0 production, $\hat{\mu}_F$ can be larger than the mass of the produced particle [30] and will lead to larger cross sections with further evolved gluon PDFs.

The DL HEF resummation proposed in section 2.3 is compatible with the factorisation scheme and the evolution of the usual NLO and NNLO PDFs and correctly reproduces the LL($\ln 1/z$) terms in the CF coefficient function up to NNLO in α_s, as it was shown in sections 2.3 and 2.4. However this resummation is applicable only in the region of $z \ll 1$. Power corrections $\mathcal{O}(z)$ to the CF coefficient function are missing in the HEF calculation with any N^{k}LL accuracy, while they are equally importantas the logarithmic terms at $z \sim 1$. For the value of the total cross section, the whole range of z from 0 to 1 contributes due to the integration over z in eq. (1.1). In the following subsections, we will propose two approaches to match these DL HEF and NLO CF results in z space and will compare the corresponding numerical results.

3.1 The subtractive-matching prescription

The simplest matching prescription between NLO CF and DLA HEF calculations consists in the subtraction of the $z \to 0$ asymptotics of the NLO CF coefficient function, to avoid double-counting it with the HEF contribution:

$$\sigma_{\text{NLO+HEF}}^{[m]} = \sigma_{\text{LO CF}}^{[m]} + \sum_{i,j=q,\bar{q},g} \int_{z_{\min}}^{1} \frac{dz}{z} \left[\check{\sigma}_{\text{HEF}}^{[m],ij}(z) + \hat{\sigma}_{\text{NLO CF}}^{[m],ij}(z) - \hat{\sigma}_{\text{NLO CF}}^{[m],ij}(0) \right] \mathcal{L}_{ij}(z), \quad (3.1)$$

where $\check{\sigma}_{\text{HEF}}^{[m],gg}$ is defined in eq. (2.7) while, for other partonic channels, $\check{\sigma}_{\text{HEF}}^{[m],ij} = \hat{\sigma}_{\text{HEF}}^{[m],ij}$ and $\hat{\sigma}_{\text{NLO CF}}^{[m],ij}(z)$ includes only the $\mathcal{O}(\alpha_s)$ CF terms from the original papers [28, 29].

The corresponding numerical results for $Q\bar{Q}[^1S_0^{(1)}]$ states with masses of 3 and 9.4 GeV are shown in the figure 4. One can see that the high-energy instability of the NLO cross section has gone away and the ratio of the matched cross section to the LO one becomes almost constant at high energy, which signal that energy dependence is now mostly driven by the PDFs, not by the hard-scattering coefficient.

3.2 The inverse-error-weighting matching

The InEW matching method has been proposed in ref. [53] to match the $|\mathbf{p}_{Tl^+l^-}|$ spectrum of Drell-Yan lepton pairs predicted by the TMD factorisation for $|\mathbf{p}_{Tl^+l^-}| \ll M_{l^+l^-}$ with the NLO CF calculation of the same spectrum, which is free from large logarithms of $|\mathbf{p}_{Tl^+l^-}|/M_{l^+l^-}$ for $|\mathbf{p}_{Tl^+l^-}| \gtrsim M_{l^+l^-}$. Following the same ideas, we introduce smooth weight functions $w_{\text{HEF}}(z)$ and $w_{\text{CF}}(z)$ into our cross section formula as follows:

$$\sigma_{\text{NLO+HEF}}^{[m]} = \sigma_{\text{LO CF}}^{[m]} + \qquad\qquad\qquad\qquad\qquad\qquad\qquad\qquad (3.2)$$

$$+ \sum_{i,j=q,\bar{q},g} \int_{z_{\min}}^{1} dz \quad \left\{ \left[\check{\sigma}_{\text{HEF}}^{[m],ij}(z) \frac{\mathcal{L}_{ij}(z)}{z} \right] w_{\text{HEF}}^{ij}(z) + \left[\hat{\sigma}_{\text{NLO CF}}^{[m],ij}(z) \frac{\mathcal{L}_{ij}(z)}{z} \right] w_{\text{CF}}^{ij}(z) \right\},$$
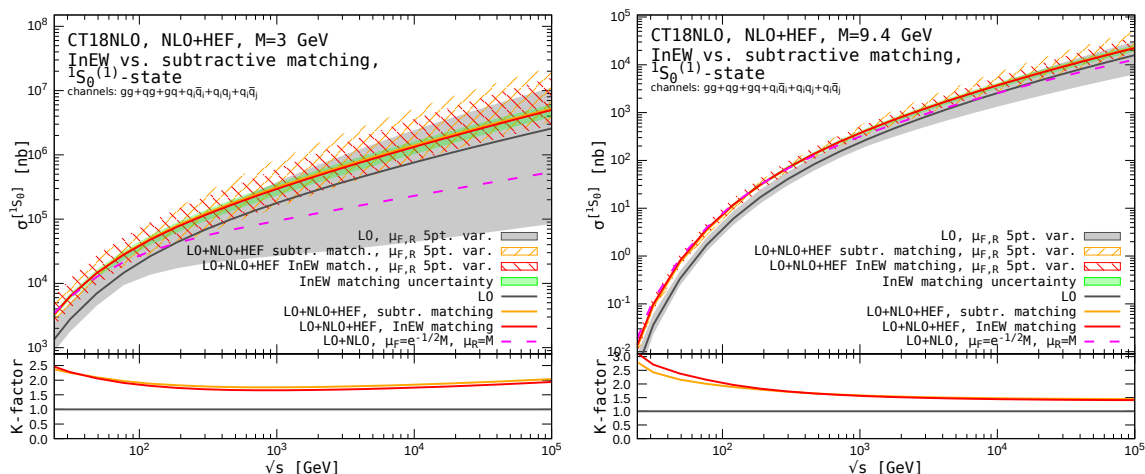
Figure 4. Comparison of the energy dependence of the hadroproduction cross sections of a $Q\bar{Q}[^1S_0^{[1]}]$ state with $M = 3\,\mathrm{GeV}$ (*left panel*) and $M = 9.4\,\mathrm{GeV}$ (*right panel*) for the matched NLO CF + DLA HEF calculations using the subtractive (orange curve and right-shaded band) and InEW matchings (red curve and left-shaded band). The dashed line depicts the central prediction of the NLO calculation using the $\hat{\mu}_F$ prescription (equation (1.4)) [30]. The LDME $\langle \mathcal{O}[^1S_0^{[1]}]\rangle$ was set to $1\,\mathrm{GeV}^3$.

where we emphasise that the weights are introduced on the level of the z integrand of the cross section, so that the distributions $1/(1-z)_+$ and $\ln(1-z)/(1-z)_+$, contained in the $\hat{\sigma}_{\mathrm{NLO\ CF},ij}^{[m]}$, have already "acted" on the function $\mathcal{L}_{ij}(z)/z$. The weights should suppress one of the contributions in the region where it is unreliable, so naturally they are chosen to be proportional to the inverse squared errors of each contribution and to add up to one:

$$w_{\mathrm{HEF}}^{ij}(z) = \frac{[\Delta\sigma_{\mathrm{HEF}}^{ij}(z)]^{-2}}{[\Delta\sigma_{\mathrm{HEF}}^{ij}(z)]^{-2} + [\Delta\sigma_{\mathrm{CF}}^{ij}(z)]^{-2}}, \ w_{\mathrm{CF}}^{ij}(z) = 1 - w_{\mathrm{HEF}}^{ij}(z), \tag{3.3}$$

where, by $\Delta\sigma_{\mathrm{HEF/CF}}^{ij}$, we refer to an estimate of the theoretical uncertainty of the corresponding contributions to the z integrand of the total cross section, which should correctly capture the fact that the HEF or the CF contributions respectively become unreliable in the $z \to 1$ or $z \to 0$ limits. The integrand uncertainty due to the matching procedure then follows from:

$$\Delta\sigma_{\mathrm{Match.}}^{ij}(z) = \left([\Delta\sigma_{\mathrm{HEF}}^{ij}(z)]^{-2} + [\Delta\sigma_{\mathrm{CF}}^{ij}(z)]^{-2}\right)^{-1/2}, \tag{3.4}$$

which, upon integration over z, gives the total cross section uncertainty due to matching procedure.

The errors entering eqs. (3.3) and (3.4) can be estimated as follows. The NLO CF cross section contains no information about the small-z behaviour of $\hat{\sigma}^{[m],ij}(z)$ beyond $\mathcal{O}(\alpha_s)$, while the LL HEF calculation provides the $\alpha_s^2 \ln 1/z$ and higher-order LLA terms. Hence one can take the $\mathcal{O}(\alpha_s^2)$ expansion of the HEF cross section, obtained in section 2.4 as an estimate for the error of the NLO CF integrand. We should also take into account the fact, that the constant $\mathcal{O}(\alpha_s^2)$ term of the $z \to 0$ asymptotics of the CF coefficient function can not be obtained from the LL HEF calculation, because it belongs to the NLL

approximation of the HEF. We estimate the coefficient in front of this term as equal to 1 and treat it as an independent source of uncertainty. Adding the constant term to the $\alpha_s^2 \log 1/z$ contribution in quadrature we obtain the following uncertainty estimate for the NLO CF contribution:

$$\Delta\sigma_{\text{CF}}^{ij}(z) = \alpha_s^2 \sigma_0^{[m]} \frac{\mathcal{L}_{ij}(z)}{z} \sqrt{\left[\frac{C_{\text{LL}}^{ij}}{\pi} \ln\frac{1}{z}\right]^2 + 1}, \tag{3.5}$$

where

$$C_{LL}^{gg} = C_A^2 \left[2A_2 + B_2 + 4A_1 \ln\frac{M^2}{\mu_F^2} + 2A_0 \ln^2\frac{M^2}{\mu_F^2}\right], \tag{3.6}$$

$$C_{LL}^{qg} = C_A C_F \left[A_2 + B_2 + 3A_1 \ln\frac{M^2}{\mu_F^2} + \frac{3}{2}A_0 \ln^2\frac{M^2}{\mu_F^2}\right], \tag{3.7}$$

$$C_{LL}^{q\bar{q}} = C_F^2 \left[B_2 + 2A_1 \ln\frac{M^2}{\mu_F^2} + A_0 \ln^2\frac{M^2}{\mu_F^2}\right], \tag{3.8}$$

and the coefficients A_0, $A_{1,2}$, B_2 can be found in table 1.

Conversely, the HEF result is valid only at $z \ll 1$ and contains no information about the $\mathcal{O}(z)$ power corrections to the CF coefficient function. On the other hand, the NLO CF coefficient function is an exact function of z at NLO in α_s. Hence one can take the NLO CF hard-scattering coefficient with its $z \to 0$ asymptotics subtracted, as an estimate of the missing $\mathcal{O}(z)$ power corrections in HEF, i.e. of the error of the latter. We also take into account the unknown $z \to 1$ asymptotics of the NNLO CF coefficient function as $\mathcal{O}(\alpha_s^2)$ term and add this estimate to the total error of the HEF contribution in quadrature as follows:

$$\Delta\sigma_{\text{HEF}}^{ij}(z) = \sqrt{\left[\left(\hat{\sigma}_{\text{NLO CF}}^{[m],ij}(z) - \hat{\sigma}_{\text{NLO CF}}^{[m],ij}(0)\right) \frac{\mathcal{L}_{ij}(z)}{z}\right]^2 + \left[\alpha_s^2 \sigma_0^{[m]} \frac{\mathcal{L}_{ij}(z)}{z}\right]^2}. \tag{3.9}$$

Using formulas (3.5) and (3.9), one can construct weights w_{CF} and w_{HEF} with the expected behaviour: e.g. $w_{\text{CF}}^{(gg)}(z)$ increases between 0 and 1 when $z \to 1$, figure 5. The latter property is ensured by the behaviour of errors (3.5) and (3.9). The CF error (3.5) increases towards $z \to 0$, while the HEF error (3.9) increases towards $z = 1$. Among three weights shown in the figure 5, only the weight for $q\bar{q}$ channel does not reach 1 when $z \to 1$. This behaviour is expectable because the NLO coefficient function, and hence the error (3.9) has no $\ln(1 - z)$ enhancement at $z \to 1$ for this channel, compared to other channels. However this feature of the weight function of the $q\bar{q}$ channel is not important numerically because the $q\bar{q}$ contribution amounts to $\mathcal{O}(1\%)$ of the total cross section at high energy.

In figures 6, 7 and 8 several plots of the z integrand of eq. (3.2) are shown as red solid lines, using weights obtained above. One can see that the InEW procedure provides a smooth interpolation between the HEF curves at $z \ll 1$ and the CF curves at z closer to 1.

The corresponding curves for the subtractive matching are shown for comparison by the red dotted lines. From figures 6, 7 and 8, the problem of the subtractive matching is evident: it subtracts the $z \to 0$ asymptotics of the NLO CF coefficient function at all
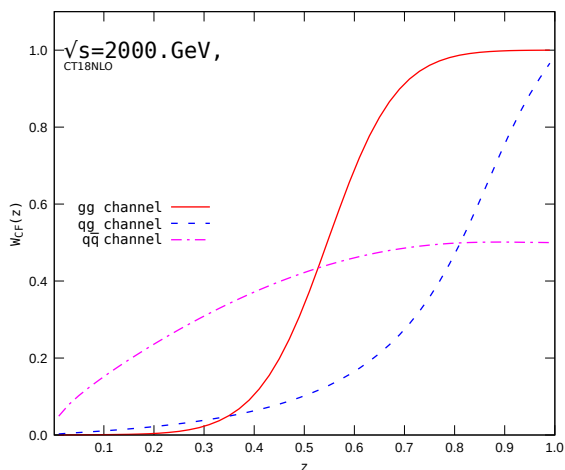
Figure 5. Plots of the InEW weights of the CF contribution for different channels as function of z with $\mu_F = \mu_R = M$.
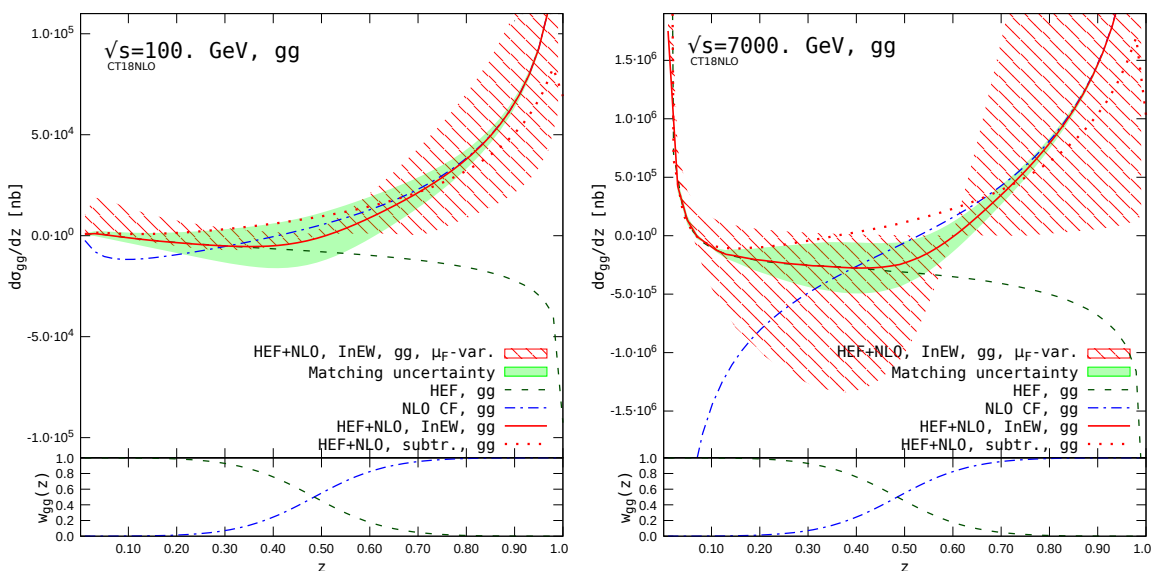

Figure 6. Matching plots for the *gg*-channel contribution to the $^1S_0^{[1]}$-state hadroproduction with $M = 3\,\text{GeV}$. The solid curve depicts the z-integrand of eq. (3.2), the dashed curve the HEF contribution (without the InEW weight), the dash-dotted curve the NLO CF contribution (without the InEW weight), and the dotted red line the integrand of eq. (3.1), i.e. the result of the subtractive matching prescription for comparison. The plots of the InEW weights are shown in the bottom inset, while the matching uncertainty (3.4) is shown as the solid band. The LDME $\langle \mathcal{O}[^1S_0^{[1]}]\rangle$ was set to $1\,\text{GeV}^3$.

values of z, thus introducing the unphysical modification of the $z \to 1$ behaviour. The InEW matching, on the other hand, smoothly connects the asymptotic regions.

The results for the matched cross section in the InEW procedure are shown by red solid curves on figure 4. The matching uncertainty, estimated by eq. (3.4) is shown separately as the green solid band in the figure 4 and it is significantly smaller than the residual scale
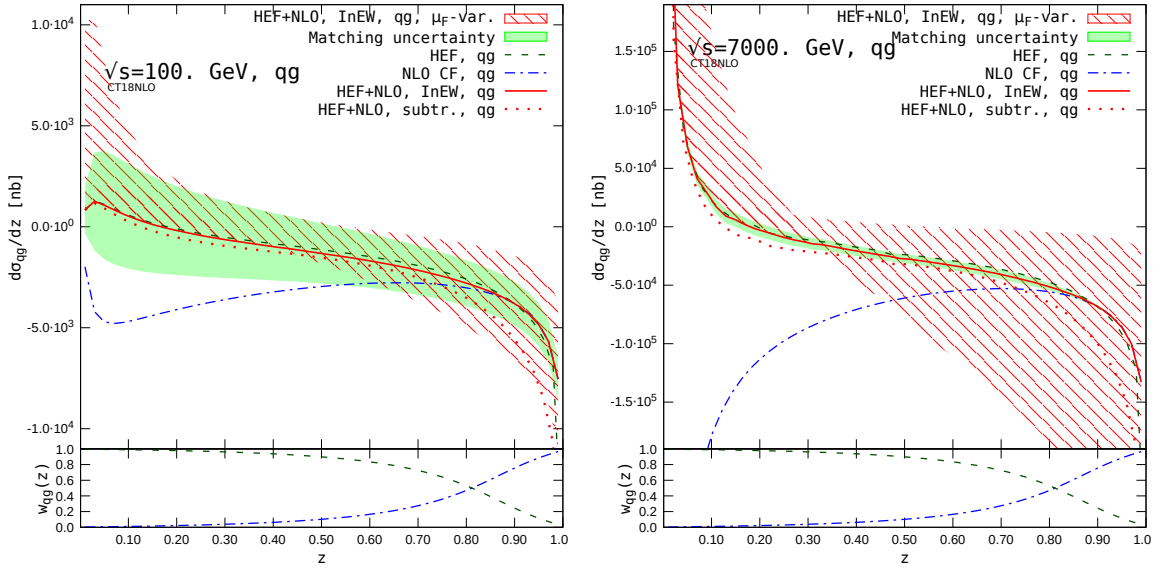
Figure 7. Matching plots for qg-channel to the $^1S_0^{[1]}$-state hadroproduction with $M = 3\,\mathrm{GeV}$. The integrand of eq. (3.1), i.e. subtractive matching prescription is shown for comparison by the dotted red line. The plots of InEW weights are shown in the bottom inset, while the matching uncertainty (3.4) is shown as the solid band. The LDME $\langle \mathcal{O}[^1S_0^{[1]}]\rangle$ was set to $1\,\mathrm{GeV}^3$.
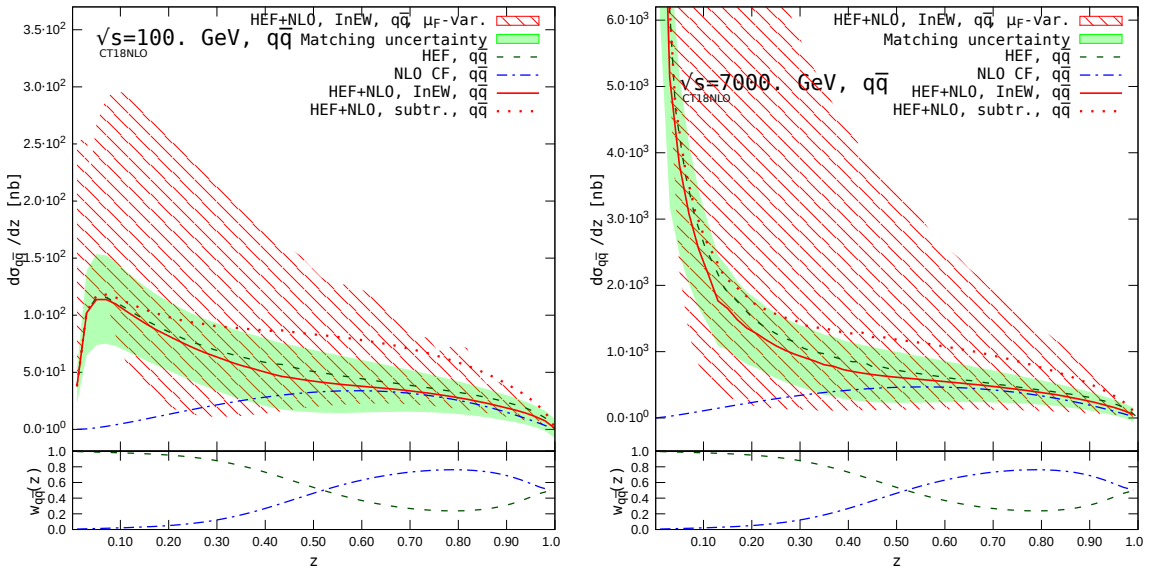
Figure 8. Matching plots for $q\bar{q}$-channel to the $^1S_0^{[1]}$-state hadroproduction with $M = 3\,\mathrm{GeV}$. The integrand of eq. (3.1), i.e. subtractive matching prescription is shown for comparison by the dotted red line. The plots of InEW weights are shown in the bottom inset, while the matching uncertainty (3.4) is shown as the solid band. The LDME $\langle \mathcal{O}[^1S_0^{[1]}]\rangle$ was set to $1\,\mathrm{GeV}^3$.
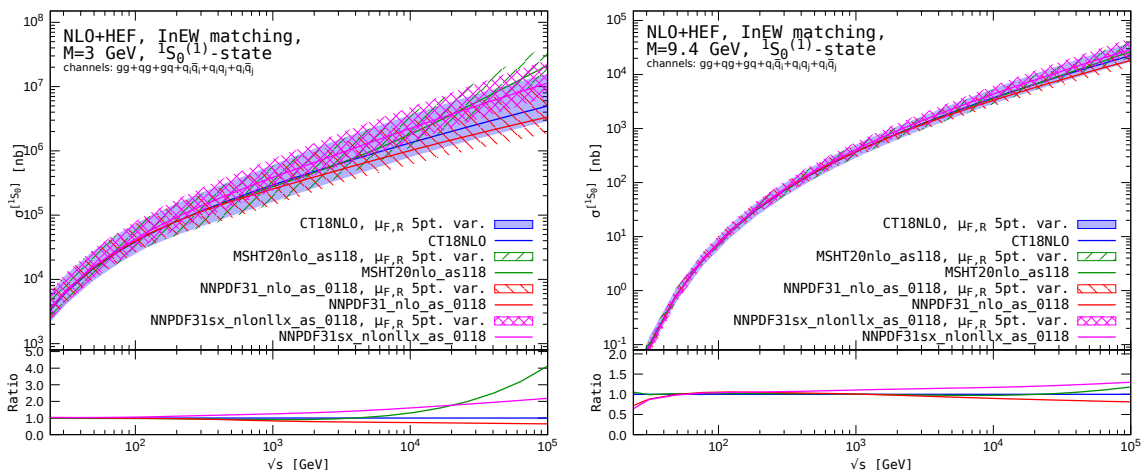
Figure 9. Dependence of the matched cross section on the choice of collinear PDF. The LDME $\langle \mathcal{O}[{}^1S_0^{(1)}]\rangle$ was set to $1\,\mathrm{GeV}^3$.

uncertainty, shown as the shaded band. The scale uncertainty band is slightly smaller in the InEW matching case.

Finally, figure 9 illustrates how the matched cross section varies depending on the choice of the collinear PDF. Since our computations are rather computer intensive, only the central members of the `CT18NLO` [82], `MSHT20nlo_as118` [83], `NNPDF31_nlo_as_0118` [84] and `NNPDF31sx_nlonllx_as_0118` [51] PDF sets, as implemented in the LHAPDF library [85] has been used for the comparison. The first three PDFs evolve according to the usual NLO DGLAP splitting functions and thus fit seamlessly into our NLO+DLA matching scheme. The last PDF set [51] contains the $\mathrm{NLL}(\ln(1/z))$ resummation and is included in figure 9 to show that the corresponding cross section, obtained in the NLO+DLA $\ln(1/z)$-resummation scheme, is consistent with the other results within uncertainties.

On one hand, figure 9 shows that there is a significant spread in the charmonium production cross sections at high energy, due to the PDF uncertainties at small values of x. At $\sqrt{s} = 13\,\mathrm{TeV}$, the central values of $\mathrm{NLO}+\mathrm{LL}(\ln(1/z))$ predictions obtained with different PDFs vary as much as by factor 1.5 up and down from our default `CT18NLO`-based estimations. This demonstrates a potential usefulness of this observable to constrain PDFs at small x. On the other hand, the theoretical uncertainties of our predictions, dominated by the scale-variation uncertainties shown in figure 9, are still larger than the spread between central curves, so to reliably discriminate between them, the scale uncertainties have to be significantly reduced which we expected to be realised once a NLL computation is available.

4 Conclusions and outlook

In the present paper, we have performed an exploratory study of the effects of High-Energy resummation on heavy-quarkonium hadroproduction cross sections. We have introduced the DLA for the resummation contributions, which is consistent with the fixed-order DGLAP evolution of PDFs and have shown that matching the NLO CF and the DL

resummed HEF results solves the problem of the negative NLO CF cross sections at high energy. This opens up the possibility to use this observable to constrain PDFs at small-x. However the scale uncertainties of our predictions have to be significantly reduced. To this end, advancing such calculation to a complete NLO+NLL($\ln(1/z)$) accuracy is required, which is a work in progress. We also emphasize that performing the matching between NLO CF and HEF contributions in z-space (as opposed to matching in Mellin-conjugate N-space, as in ref. [46]) is a simple and flexible procedure which allows one to estimate the uncertainty of the cross section due to the matching. When the NLL($\ln(1/z)$) calculation in HEF becomes available, it will be easy to match it with the NLO or possibly even NNLO CF results using the z-space technique.

Acknowledgments

A Numerics in z-space

A.1 Method 1: regularised resummation factor

This method is based on the following regularised form of the resummation factor, where the small-$\mathbf{q}_T$ oscillations are replaced by a constant in $\mathbf{q}_T$-behaviour for $\mathbf{q}_T^2 < \mathbf{q}_{T0}^2$ in such a way that the normalisation condition (2.31) still holds exactly:

$$\widetilde{\mathcal{C}}_{gg}^{\,\mathrm{DLA}}(z, \mathbf{q}_T^2, \mu_F^2) = \begin{cases} \frac{1}{\mathbf{q}_{T0}^2}\left[\delta(1-z) - \mathcal{F}\left(\frac{\mathbf{q}_{T0}^2}{\mu_F^2}, z\right)\right], & \text{if } \mathbf{q}_T^2 < \mathbf{q}_{T0}^2, \\ \mathcal{C}_{gg}^{\mathrm{DLA}}(z, \mathbf{q}_T^2, \mu_F^2), & \text{if } \mathbf{q}_T^2 > \mathbf{q}_{T0}^2, \end{cases} \tag{A.1}$$

where

$$\mathcal{F}\left(\frac{\mathbf{q}_{T0}^2}{\mu_F^2}, z\right) = \int\limits_0^{L_{\max}} dL\, J_0\left(2\sqrt{L \ln\frac{1}{z}}\right) = L_{\max}\, {}_0\tilde{F}_1\left(2, -L_{\max}\ln\frac{1}{z}\right), \tag{A.2}$$

with $L_{\max} = \hat{\alpha}_s \ln(\mathbf{q}_{T0}^2/\mu_F^2)$ and ${}_0\tilde{F}_1$, which is the regularised confluent hypergeometric function. In the $\mathbf{q}_{T0}^2 \to 0$ limit, the function $\mathcal{F}$ turns into $\delta(1-z)$ but this limit is approached very slowly. So, for all reasonable values of $|\mathbf{q}_{T0}|$, even as small as $10^{-3}\,\mathrm{GeV}$,

the function (A.2) is still rather smoothly dependent on z and does not cause any numerical problems. For the quark-induced channel, the regularised resummation factor:

$$\widetilde{\mathcal{C}}_{gq}^{\text{DLA}}(z, \mathbf{q}_T^2, \mu_F^2) = \frac{C_F}{C_A} \begin{cases} -\frac{1}{\mathbf{q}_{T0}^2} \mathcal{F}\left(\frac{\mathbf{q}_{T0}^2}{\mu_F^2}, z\right), & \text{if } \mathbf{q}_T^2 < \mathbf{q}_{T0}^2, \\ \mathcal{C}_{gg}^{\text{DLA}}(z, \mathbf{q}_T^2, \mu_F^2), & \text{if } \mathbf{q}_T^2 > \mathbf{q}_{T0}^2, \end{cases} \tag{A.3}$$

satisfies the normalisation condition (2.32).

After substituting the regularised resummation factors (A.1) or (A.3) into eq. (2.6), one splits the $\mathbf{q}_{T1,2}^2$-integrations into regions with $\mathbf{q}_{T1,2}^2 < \mathbf{q}_{T0}^2$ and $\mathbf{q}_{T1,2}^2 > \mathbf{q}_{T0}^2$. If, for example $\mathbf{q}_{T1}^2 < \mathbf{q}_{T0}^2$, then this transverse momentum can be neglected in all the rest of the integrand in eq. (2.6) because the dependence of the HEF coefficient function as well as the dependence of the factor $1/M_T^4$ on $\mathbf{q}_{T1}^2$ is smooth. This approximation allows one to trivially integrate out $\mathbf{q}_{T1}^2$ in the region $\mathbf{q}_{T1}^2 < \mathbf{q}_{T0}^2$ introducing the error which scales as $\mathcal{O}(\mathbf{q}_{T0}^2/M^2)$ and can be made negligible by choosing a reasonably small value of $\mathbf{q}_{T0}^2$. In the region $\mathbf{q}_{T1}^2 > \mathbf{q}_{T0}^2$ no approximations are made. The $\mathbf{q}_{T2}^2$-integration can be decomposed in the same manner and the region where both $\mathbf{q}_{T1}^2 < \mathbf{q}_{T0}^2$ and $\mathbf{q}_{T2}^2 < \mathbf{q}_{T0}^2$ produces the LO CF term in eq. (2.7), while the LO-subtracted partonic cross section in the method under consideration is decomposed as follows:

$$\check{\sigma}_{gg}^{[m], \text{ HEF}} = \check{\sigma}_{2\text{UI}}^{[m]} + \check{\sigma}_{2\text{F}}^{[m]} + 2\left[\check{\sigma}_{1\text{UI}-\text{C}}^{[m]} - \check{\sigma}_{1\text{UI}-\text{CF}}^{[m]} - \check{\sigma}_{\text{F}}^{[m]}\right], \tag{A.4}$$

where the separate contributions depend on the value of the cut $\mathbf{q}_{T0}$ but this dependence should cancel in their sum for sufficiently small $\mathbf{q}_{T0}^2 \ll M^2$. For the quark-induced channels, the resummed partonic coefficient can be calculated in terms of the same contributions as:

$$\hat{\sigma}_{gq}^{[m], \text{ HEF}} = \frac{C_F}{C_A}\left[\check{\sigma}_{2\text{UI}}^{[m]} + \check{\sigma}_{2\text{F}}^{[m]} + \check{\sigma}_{1\text{UI}-\text{C}}^{[m]} - 2\check{\sigma}_{1\text{UI}-\text{CF}}^{[m]} - \check{\sigma}_{\text{F}}^{[m]}\right], \tag{A.5}$$

$$\hat{\sigma}_{q\bar{q}}^{[m], \text{ HEF}} = \left(\frac{C_F}{C_A}\right)^2\left[\check{\sigma}_{2\text{UI}}^{[m]} + \check{\sigma}_{2\text{F}}^{[m]} - 2\check{\sigma}_{1\text{UI}-\text{CF}}^{[m]}\right]. \tag{A.6}$$

The *doubly-unintegrated* contribution, $\check{\sigma}_{2\text{UI}}^{[m]}$, entering eqs. (A.4), (A.5) and (A.6) is just eq. (2.6) with both $\mathbf{q}_{T1,2}^2 > \mathbf{q}_{T0}^2$ and the resummation factor (2.30). Other contributions

are calculated as follows:

$$
\check{\sigma}_{1\mathrm{UI-CF}}^{[m]} = \int\limits_{-\infty}^{+\infty} d\eta \int\limits_{\mathbf{q}_{T0}^2}^{\infty} d\mathbf{q}_{T1}^2 \mathcal{C}_{gg}^{\mathrm{DLA}}\left(\sqrt{z}\frac{M_{T1}}{M}e^\eta, \mathbf{q}_{T1}^2, \mu_F, \mu_R\right)
$$

$$
\times \mathcal{F}\left(\frac{\mathbf{q}_{T0}^2}{\mu_F^2}, \sqrt{z}\frac{M_{T1}}{M}e^{-\eta}\right) \int\limits_0^{2\pi} \frac{d\phi}{2}\, \frac{H(\mathbf{q}_{T1}^2, 0, \phi)}{M_{T1}^4}, \tag{A.7}
$$

$$
\check{\sigma}_{1\mathrm{UI-C}}^{[m]} = \int\limits_{\mathbf{q}_{T0}^2}^{\infty} d\mathbf{q}_{T1}^2\, \mathcal{C}_{gg}^{\mathrm{DLA}}\left(z\frac{M_{T1}^2}{M^2}, \mathbf{q}_{T1}^2, \mu_F, \mu_R\right) \int\limits_0^{2\pi} \frac{d\phi}{2}\, \frac{H(\mathbf{q}_{T1}^2, 0, \phi)}{M_{T1}^4}, \tag{A.8}
$$

$$
\check{\sigma}_{2\mathrm{F}}^{[m]} = \int\limits_{-\infty}^{\infty} d\eta\, \mathcal{F}\left(\frac{\mathbf{q}_{T0}^2}{\mu_F^2}, \sqrt{z}e^\eta\right) \mathcal{F}\left(\frac{\mathbf{q}_{T0}^2}{\mu_F^2}, \sqrt{z}e^{-\eta}\right) \int\limits_0^{2\pi} \frac{d\phi}{2}\, \frac{H(0, 0, \phi)}{M^4}, \tag{A.9}
$$

$$
\check{\sigma}_{\mathrm{F}}^{[m]} = \mathcal{F}\left(\frac{\mathbf{q}_{T0}^2}{\mu_F^2}, z\right) \int\limits_0^{2\pi} \frac{d\phi}{2}\, \frac{H(0, 0, \phi)}{M^4}, \tag{A.10}
$$

where $M_{T1}^2 = M^2 + \mathbf{q}_{T1}^2$.

A.2 Method 2: small-q_T subtraction

The approach described in this section has been inspired by the treatment of the same problem in the ref. [44]. The method relies on the same kind of decomposition of the transverse-momentum dependence of the integrand as in eq. (2.39), but now we perform it to isolate the LO contribution, using the normalisation condition (2.31). To save space, let us introduce the short-hand notation for the integrand of eq. (2.6):

$$
\mathcal{J}(\xi_1, \xi_2) = \mathcal{C}_{gg}\left(\sqrt{z}\frac{M_T(\xi_1, \xi_2)}{M}e^\eta, \mathbf{q}_{T1}^2, \mu_F, \mu_R\right) \mathcal{C}_{gg}\left(\sqrt{z}\frac{M_T(\xi_1, \xi_2)}{M}e^{-\eta}, \mathbf{q}_{T2}^2, \mu_F, \mu_R\right)
$$

$$
\times \frac{H(\xi_1^2 \mathbf{q}_{T1}^2, \xi_2^2 \mathbf{q}_{T2}^2, \phi)}{M_T^4(\xi_1, \xi_2)}, \tag{A.11}
$$

where $M_T^2(\xi_1, \xi_2) = M^2 + (\xi_1 \mathbf{q}_{T1} + \xi_2 \mathbf{q}_{T2})^2$ and variables $\xi_{1,2} = \{0, 1\}$ are introduced for us to be able to turn on and off the "smooth part" of the dependence of the integrand on transverse momenta, while the dependence of $\mathcal{J}$ on $\mathbf{q}_{T1,2}^2$, ϕ and η is implicit. Similarly to eq. (2.39) we decompose

$$
\mathcal{J}(1,1) = \mathcal{J}_1 + \mathcal{J}_2 + \mathcal{J}_3 + \mathcal{J}(0,0)\theta(\mu_F^2 - \mathbf{q}_{T1}^2)\theta(\mu_F^2 - \mathbf{q}_{T2}^2),
$$

where the last term of this decomposition, when substituted to eq. (2.6) gives us $\sigma_{\mathrm{LO}}^{[m]}\delta(1-z)$ due to normalisation condition (2.31), while the terms $\mathcal{J}_{1,2,3}$ are:

$$
\begin{aligned}
\mathcal{J}_1 &= \mathcal{J}(1,1) - \mathcal{J}(0,1)\theta(\mu_F^2 - \mathbf{q}_{T1}^2) \\
&\quad - \mathcal{J}(1,0)\theta(\mu_F^2 - \mathbf{q}_{T2}^2) + \mathcal{J}(0,0)\theta(\mu_F^2 - \mathbf{q}_{T1}^2)\theta(\mu_F^2 - \mathbf{q}_{T2}^2), \\
\mathcal{J}_2 &= \left[\mathcal{J}(1,0) - \mathcal{J}(0,0)\theta(\mu_F^2 - \mathbf{q}_{T1}^2)\right]\theta(\mu_F^2 - \mathbf{q}_{T2}^2), \\
\mathcal{J}_3 &= \left[\mathcal{J}(0,1) - \mathcal{J}(0,0)\theta(\mu_F^2 - \mathbf{q}_{T2}^2)\right]\theta(\mu_F^2 - \mathbf{q}_{T1}^2).
\end{aligned}
$$

Using these expressions, the *doubly-unintegrated* contribution $\check{\sigma}^{[m]}_{2\text{UI}-\text{S}}$ in this method is defined as eq. (2.6) with integrand $\mathcal{J}_1$ and without any low-$\mathbf{q}_{T1,2}$ cuts. The *single-unintegrated* contribution is obtained by substituting $\mathcal{J}_2$ into eq. (2.6) and integrating out $\mathbf{q}^2_{T2}$ via eq. (2.31):

$$
\check{\sigma}^{[m]}_{1\text{UI}-\text{S}} = \int\limits_0^\infty d\mathbf{q}^2_{T1} \int\limits_0^{2\pi} \frac{d\phi}{2} \ \left[\mathcal{C}_{gg}\left(z\frac{M^2_{T1}}{M^2}, \mathbf{q}^2_{T1}, \mu^2_F, \mu^2_R \right) \frac{H(\mathbf{q}^2_{T1}, 0, \phi)}{M^4_{T1}} \right.
$$
$$
\left. - \mathcal{C}_{gg}\left(z, \mathbf{q}^2_{T1}, \mu^2_F, \mu^2_R \right) \frac{H(0,0,\phi)}{M^4}\theta(\mu^2_F - \mathbf{q}^2_{T1}) \right]. \quad \text{(A.12)}
$$

The LO subtracted resummed cross section for the *gg* channel is calculated as:

$$
\check{\sigma}^{[m],\ \text{HEF}}_{gg} = \check{\sigma}^{[m]}_{2\text{UI}-\text{S}} + 2\check{\sigma}^{[m]}_{1\text{UI}-\text{S}}, \quad \text{(A.13)}
$$

while, for the quark-induced channels, one has:

$$
\hat{\sigma}^{[m],\ \text{HEF}}_{gq} = \frac{C_F}{C_A}\left[\check{\sigma}^{[m]}_{2\text{UI}-\text{S}} + \check{\sigma}^{[m]}_{1\text{UI}-\text{S}} \right], \quad \text{(A.14)}
$$

$$
\hat{\sigma}^{[m],\ \text{HEF}}_{q\bar{q}} = \left(\frac{C_F}{C_A} \right)^2 \check{\sigma}^{[m]}_{2\text{UI}-\text{S}}. \quad \text{(A.15)}
$$

For the DLA resummation factor, the numerical results obtained in both methods agree within the integration accuracy. However, the subtraction method allows one to work with resummation factor given in the numerical form. The only requirement is that it should satisfy the normalisation condition (2.31), which is true for example for the resummation factor (2.18) with full LL($\ln(1/z)$) anomalous dimension, obtained as numerical solution of eq. (2.19), but with $R(\gamma) = 1$, as discussed in appendix B, or for the Gaussian-smeared resummation factor discussed in appendix C.

B Effects of the anomalous dimension beyond LO

In this appendix, we study the effects of terms beyond LO in α_s in the anomalous dimension (2.20) on the resummed cross section, while still omitting the scheme-transformation factor $R(\gamma)$ from the eq. (2.18). We have obtained the numerical solution of eq. (2.19), which in terms of the variable $\rho = N/\hat{\alpha}_s$ has the form:

$$
\chi(\gamma_{gg}(\rho)) = \rho. \quad \text{(B.1)}
$$

This equation has already been studied numerically in refs. [81, 86]. The perturbative branch of the solution has a cut-discontinuity depicted in the figure 10, and inverse Mellin transform integral (2.29) can be written as an integral over the contour in ρ-plane which should avoid crossing this cut. Our numerical results for the real and imaginary parts of the solution agree with results of ref. [81] and are also shown on figure 10.

Plots of the resummation factor resulting from the numerical inverse Mellin transform are shown on figure 11. At moderately small values of z, it is close to the DLA, but at
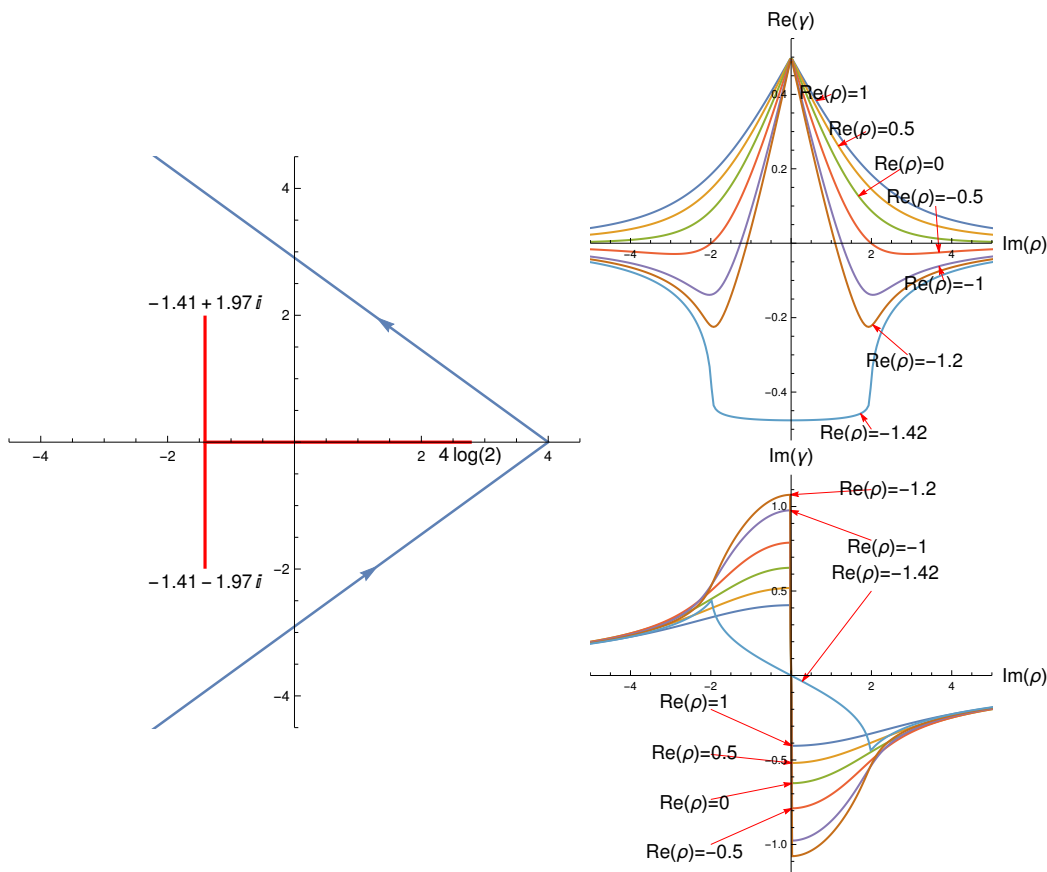
Figure 10. *Left panel:* branch cut discontinuity of the function $\gamma_{gg}(\rho)$ and the integration contour of the inverse Mellin transform in the ρ-plane. *Right panel:* real and imaginary parts of $\gamma_{gg}(\rho)$ as functions of $\mathrm{Im}\,\rho$ at fixed $\mathrm{Re}\,\rho = 1, 0.5, 0, -0.5, -1, -1.2, -1.42$. To be compared with the plots in the figure 1 of the ref. [81].

smaller values of z it deviates from DLA and the most numerically important region of $\mathbf{q}_T^2 \sim 1\,\mathrm{GeV}^2$ features a significant peak in the negative direction.

On figure 12, the $\sqrt{s}$-dependence of the HEF-resummed part of the total cross section of production of the $Q\bar{Q}[^1S_0^{(1)}]$ state in the gg channel is plotted. The central lines as well as uncertainty bands resulting from the variation of μ_F by a factor of 2 above and below the default value $\mu_F = M$ are presented. Two approximations for the resummation factor are compared on figure 12: the DLA, introduced in the section 2.3, and the approximation described above in this appendix, which includes effects beyond LO in $\gamma_{gg}(N, \alpha_s)$. The LO CF central curve and the μ_F uncertainty is also shown on figure 12 for comparison. One can see that, while DLA significantly reduces the scale uncertainty in comparison to the LO CF result, the inclusion of higher-order corrections to $\gamma_{gg}(N, \alpha_s)$ blows up the scale uncertainty at high energies so much that, for $\sqrt{s} > 4\,\mathrm{TeV}$ (left panel of the figure 12) or $\sqrt{s} > 7\,\mathrm{TeV}$ (right panel of the figure 12), the resummed part of cross section can become negative.

This catastrophic factorisation-scale uncertainty is a consequence of the mismatch between the μ_F-dependence of the resummation factor and one of the collinear PDFs used.
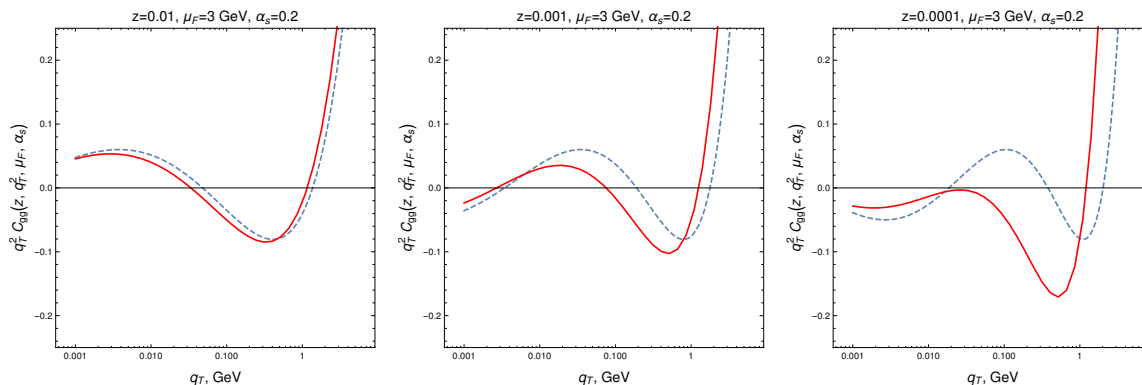
Figure 11. Resummation factor $\mathcal{C}_{gg}$ as a function of $|\mathbf{q}_T|$ for several values of z. The DLA result is plotted by the dashed curve and numerical result with $\text{LL}(\ln(1/z))$ anomalous dimension, obtained as a solution of eq. (2.19) is plotted by the solid curve.
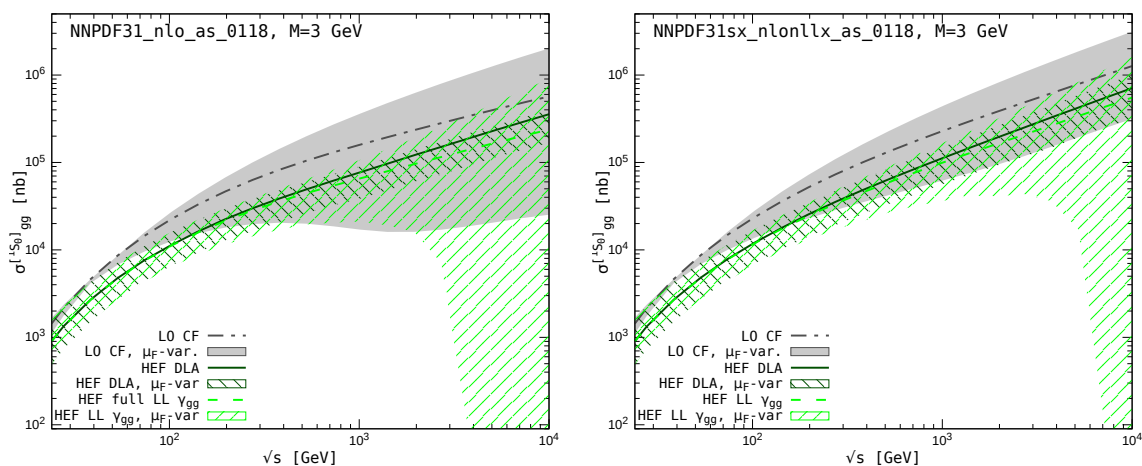

Figure 12. Energy dependence of the HEF resummed part of the cross section (LO CF included) in the gg channel: the DLA result and it's μ_F-variation are plotted as solid line and left-shaded band, dashed line and right-shaded μ_F-variation band correspond to the calculation using the full numerical solution of eq. (2.19) for $\gamma_{gg}(N, \alpha_s)$. For comparison, the LO CF cross section together with its μ_F-variation is shown by the dash-dotted line and the corresponding solid band. The gluon PDFs used are `NNPDF31_nlo_as_0118` [84](left panel) and `NNPDF31sx_nlonllx_as_0118` [51](right panel). The LDME $\langle \mathcal{O}[^1S_0^{(1)}] \rangle$ was set to $1\,\text{GeV}^3$.

For the left plot on figure 12, we have employed the central eigenset of the `NNPDF31_nlo _as_0118` [84] PDFs and, in the right panel, the $\text{NLL}(\ln(1/z))$-resummed version of the `NNPDF31` PDFs has been used [51]. Figure 12 serves as a numerical illustration of our statement in section 2.3 that one should not increase the accuracy of the resummation factors in HEF beyond DLA if collinear PDFs result from a fixed-order DGLAP evolution, as in the left plot of figure 12. In the case of the $\text{NLL}(\ln(1/z))$-resummed PDFs (right panel of figure 12), the addition of the full $\text{LL}(\ln(1/z))$ correction to γ_{gg} is also not justified because in this case the formal perturbative accuracy of the PDFs is greater that of the resummation factor and the NLL resummed version γ_{gg} is significantly [51, 87] different
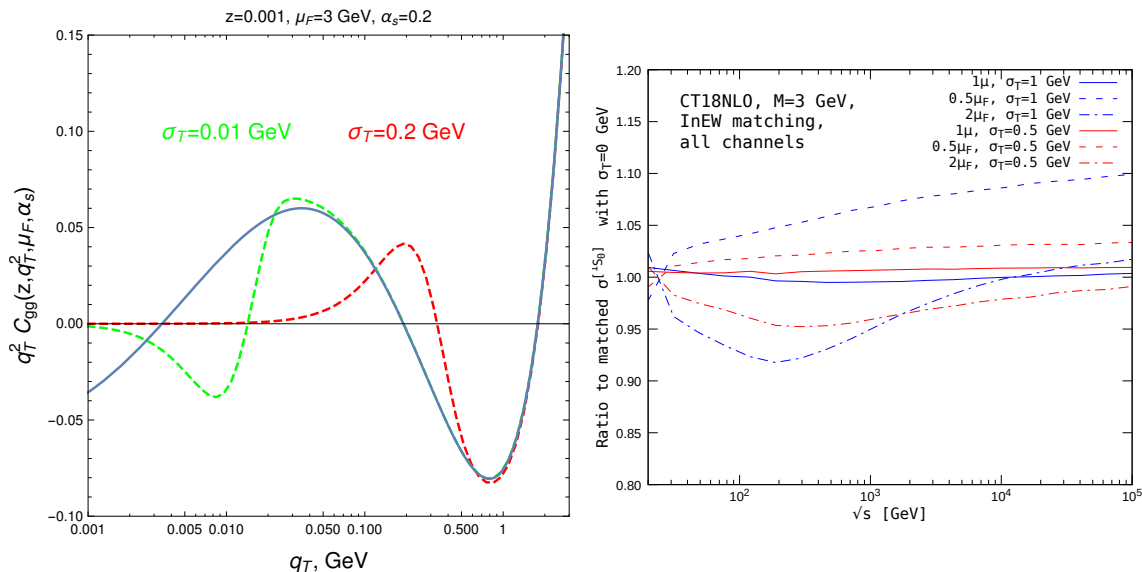
Figure 13. *Left panel:* the $\mathbf{q}_T$-dependence of the Gaussian smeared DLA resummation factor for two values of σ_T (dashed curves). The DLA resummation factor without smearing (2.30) is shown by solid curve for comparison. *Right panel:* the energy-dependence of the ratio of the matched cross section obtained in the DLA with Gaussian smearing with $\sigma_T = 0.5$ and $1\,\mathrm{GeV}$ to the result without smearing and its μ_F-scale variation.

from the full $\mathrm{LL}(\ln(1/z))$-resummed one, so even in this case we have a mismatch of the μ_F-dependence between the PDFs and the resummation factor.

C Higher-twist effects

It may be argued that the oscillatory behaviour of the resummation factors at $\mathbf{q}_T^2 \ll 1\,\mathrm{GeV}^2$, depicted on figure 11, is un-physical and that in this domain the resummation factor is dominated by non-perturbative effects. In this context, one would like to understand how much the total cross section depends on the detailed behaviour of the resummation factor at small values of $\mathbf{q}_T^2$. As a toy model to study this question, we have performed a convolution of the DLA resummation factor (2.28) with Gaussian of the width σ_T in transverse momentum which can be done analytically with the Mellin-space result (2.28):

$$
\mathcal{C}_{gg}^{\mathrm{DLA},\sigma}(N, \mathbf{q}_T^2, \mu_F, \mu_R) = \int \frac{d^2\mathbf{k}_T}{\pi\sigma_T^2} \exp\left[-\frac{\mathbf{k}_T^2}{\sigma_T^2}\right] \mathcal{C}_{gg}^{\mathrm{DLA}}(N, (\mathbf{q}_T + \mathbf{k}_T)^2, \mu_F, \mu_R)
$$
$$
= \frac{1}{\sigma_T^2}\left(\frac{\sigma_T^2}{\mu_F^2}\right)^{\gamma_N} e^{-\frac{\mathbf{q}_T^2}{\sigma_T^2}} {}_1F_1\left(\gamma_N, 1, \frac{\mathbf{q}_T^2}{\sigma_T^2}\right), \tag{C.1}
$$

and then converted it to the z-space numerically. Eq. (C.1) still satisfies the normalisation condition (2.31) up to corrections suppressed as $e^{-\mu_F^2/\sigma_T^2}$, so the method from the section A.2 can be used to calculate the cross section if $\sigma_T \lesssim 1\,\mathrm{GeV}$. Several plots of the $|\mathbf{q}_T|$-dependence of the smeared resummation factor (C.1), transformed numerically to the z-space are presented in the left panel of figure 13.

In the right panel of figure 13, the ratio of the matched cross section obtained with the Gaussian-smeared resummation factor to the cross section without $\mathbf{k}_T$-smearing is plotted as a function of $\sqrt{s}$ for $\sigma_T = 0.5$ and $1\,\mathrm{GeV}$. The results with $\sigma_T = 0.5$ and $1\,\mathrm{GeV}$ differ from the matched cross section calculated without a Gaussian by at most ten percent for $\mu_F = 0.5M$ and $2M$, while the results at the default scale are even closer.

From the detailed consideration of the small-$\mathbf{q}_T$ subtraction method, described in section A.2, one can see that the effect of the $\mathbf{k}_T$-smearing on the total cross section is suppressed as $\mathcal{O}(\sigma_T^2/M^2) \sim O(\Lambda_{\mathrm{QCD}}^2/M^2)$ if $\sigma_T \sim \Lambda_{QCD}$. In other words, these effect follow a subleading power in our hard scale M; it is a *higher-twist effect*.

The width of the "intrinsic" $\mathbf{k}_T$-distribution is expected to be increasing with energy, due to increasing saturation scale (see e.g. ref. [88] and references therein), so that, at high enough energies, the twist expansion will completely break down due to the effect discussed above. However, as one can see from figure 13 this effects are unlikely to be the main source of uncertainty in our calculation at LHC energies and even beyond.

Open Access. This article is distributed under the terms of the Creative Commons Attribution License ([CC-BY 4.0](https://creativecommons.org/licenses/by/4.0/)), which permits any use, distribution and reproduction in any medium, provided the original author(s) and source are credited.

References

[1] E. Chapon et al., *Prospects for quarkonium studies at the high-luminosity LHC*, *Prog. Part. Nucl. Phys.* **122** (2022) 103906 [arXiv:2012.14161] [INSPIRE].

[2] A. Arbuzov et al., *On the physics potential to study the gluon content of proton and deuteron at NICA SPD*, *Prog. Part. Nucl. Phys.* **119** (2021) 103858 [arXiv:2011.15005] [INSPIRE].

[3] J.-P. Lansberg, *New observables in inclusive production of quarkonia*, *Phys. Rept.* **889** (2020) 1 [arXiv:1903.09185] [INSPIRE].

[4] N. Brambilla et al., *QCD and strongly coupled gauge theories: challenges and perspectives*, *Eur. Phys. J. C* **74** (2014) 2981 [arXiv:1404.3723] [INSPIRE].

[5] N. Brambilla et al., *Heavy quarkonium: progress, puzzles, and opportunities*, *Eur. Phys. J. C* **71** (2011) 1534 [arXiv:1010.5827] [INSPIRE].

[6] G.T. Bodwin, E. Braaten and G.P. Lepage, *Rigorous QCD analysis of inclusive annihilation and production of heavy quarkonium*, *Phys. Rev. D* **51** (1995) 1125 [*Erratum ibid.* **55** (1997) 5853] [hep-ph/9407339] [INSPIRE].

[7] M. Butenschoen and B.A. Kniehl, *Reconciling J/ψ production at HERA, RHIC, Tevatron, and LHC with NRQCD factorization at next-to-leading order*, *Phys. Rev. Lett.* **106** (2011) 022003 [arXiv:1009.5662] [INSPIRE].

[8] M. Butenschoen and B.A. Kniehl, *World data of J/ψ production consolidate NRQCD factorization at NLO*, *Phys. Rev. D* **84** (2011) 051501 [arXiv:1105.0820] [INSPIRE].

[9] M. Butenschoen and B.A. Kniehl, *J/ψ polarization at Tevatron and LHC: nonrelativistic-QCD factorization at the crossroads*, *Phys. Rev. Lett.* **108** (2012) 172002 [arXiv:1201.1872] [INSPIRE].

[10] M. Butenschoen and B.A. Kniehl, *Next-to-leading-order tests of NRQCD factorization with J/ψ yield and polarization*, *Mod. Phys. Lett. A* **28** (2013) 1350027 [`arXiv:1212.2037`] [ɪɴSPIRE].

[11] K.-T. Chao, Y.-Q. Ma, H.-S. Shao, K. Wang and Y.-J. Zhang, *J/ψ polarization at hadron colliders in nonrelativistic QCD*, *Phys. Rev. Lett.* **108** (2012) 242004 [`arXiv:1201.2675`] [ɪɴSPIRE].

[12] B. Gong, L.-P. Wan, J.-X. Wang and H.-F. Zhang, *Polarization for prompt J/ψ and ψ(2s) production at the Tevatron and LHC*, *Phys. Rev. Lett.* **110** (2013) 042002 [`arXiv:1205.6682`] [ɪɴSPIRE].

[13] G.T. Bodwin, H.S. Chung, U.-R. Kim and J. Lee, *Fragmentation contributions to J/ψ production at the Tevatron and the LHC*, *Phys. Rev. Lett.* **113** (2014) 022001 [`arXiv:1403.3612`] [ɪɴSPIRE].

[14] B. Gong, J.-X. Wang and H.-F. Zhang, *QCD corrections to Υ production via color-octet states at the Tevatron and LHC*, *Phys. Rev. D* **83** (2011) 114021 [`arXiv:1009.3839`] [ɪɴSPIRE].

[15] K. Wang, Y.-Q. Ma and K.-T. Chao, *Υ(1S) prompt production at the Tevatron and LHC in nonrelativistic QCD*, *Phys. Rev. D* **85** (2012) 114003 [`arXiv:1202.6012`] [ɪɴSPIRE].

[16] B. Gong, L.-P. Wan, J.-X. Wang and H.-F. Zhang, *Complete next-to-leading-order study on the yield and polarization of Υ(1S, 2S, 3S) at the Tevatron and LHC*, *Phys. Rev. Lett.* **112** (2014) 032001 [`arXiv:1305.0748`] [ɪɴSPIRE].

[17] M. Butenschoen, Z.-G. He and B.A. Kniehl, *ηc production at the LHC challenges nonrelativistic-QCD factorization*, *Phys. Rev. Lett.* **114** (2015) 092004 [`arXiv:1411.5287`] [ɪɴSPIRE].

[18] V.D. Barger, W.-Y. Keung and R.J.N. Phillips, *On ψ and Υ production via gluons*, *Phys. Lett. B* **91** (1980) 253 [ɪɴSPIRE].

[19] V.D. Barger, W.-Y. Keung and R.J.N. Phillips, *Hadroproduction of ψ and Υ*, *Z. Phys. C* **6** (1980) 169 [ɪɴSPIRE].

[20] R. Gavai, D. Kharzeev, H. Satz, G.A. Schuler, K. Sridhar and R. Vogt, *Quarkonium production in hadronic collisions*, *Int. J. Mod. Phys. A* **10** (1995) 3043 [`hep-ph/9502270`] [ɪɴSPIRE].

[21] Y.-Q. Ma and R. Vogt, *Quarkonium production in an improved color evaporation model*, *Phys. Rev. D* **94** (2016) 114029 [`arXiv:1609.06042`] [ɪɴSPIRE].

[22] J.-P. Lansberg, H.-S. Shao, N. Yamanaka, Y.-J. Zhang and C. Noûs, *Complete NLO QCD study of single- and double-quarkonium hadroproduction in the colour-evaporation model at the Tevatron and the LHC*, *Phys. Lett. B* **807** (2020) 135559 [`arXiv:2004.14345`] [ɪɴSPIRE].

[23] N. Brambilla, H.S. Chung and A. Vairo, *Inclusive production of heavy quarkonia in pNRQCD*, *JHEP* **09** (2021) 032 [`arXiv:2106.09417`] [ɪɴSPIRE].

[24] Y.-Q. Ma and K.-T. Chao, *New factorization theory for heavy quarkonium production and decay*, *Phys. Rev. D* **100** (2019) 094007 [`arXiv:1703.08402`] [ɪɴSPIRE].

[25] R. Li, Y. Feng and Y.-Q. Ma, *Exclusive quarkonium production or decay in soft gluon factorization*, *JHEP* **05** (2020) 009 [`arXiv:1911.05886`] [ɪɴSPIRE].

[26] A.-P. Chen and Y.-Q. Ma, *Theory for quarkonium: from NRQCD factorization to soft gluon factorization*, *Chin. Phys. C* **45** (2021) 013118 [arXiv:2005.08786] [InSPIRE].

[27] Z.-B. Kang, J.-W. Qiu and G. Sterman, *Heavy quarkonium production and polarization*, *Phys. Rev. Lett.* **108** (2012) 102002 [arXiv:1109.1520] [InSPIRE].

[28] J.H. Kühn and E. Mirkes, *QCD corrections to toponium production at hadron colliders*, *Phys. Rev. D* **48** (1993) 179 [hep-ph/9301204] [InSPIRE].

[29] A. Petrelli, M. Cacciari, M. Greco, F. Maltoni and M.L. Mangano, *NLO production and decay of quarkonium*, *Nucl. Phys. B* **514** (1998) 245 [hep-ph/9707223] [InSPIRE].

[30] J.-P. Lansberg and M.A. Ozcelik, *Curing the unphysical behaviour of NLO quarkonium production at the LHC and its relevance to constrain the gluon PDF at low scales*, *Eur. Phys. J. C* **81** (2021) 497 [arXiv:2012.00702] [InSPIRE].

[31] G.A. Schuler, *Quarkonium production and decays*, Ph.D. thesis, Hamburg U., Hamburg, Germany (1994) [hep-ph/9403387] [InSPIRE].

[32] M.L. Mangano and A. Petrelli, *NLO quarkonium production in hadronic collisions*, *Int. J. Mod. Phys. A* **12** (1997) 3887 [hep-ph/9610364] [InSPIRE].

[33] Y. Feng, J.-P. Lansberg and J.-X. Wang, *Energy dependence of direct-quarkonium production in pp collisions from fixed-target to LHC energies: complete one-loop analysis*, *Eur. Phys. J. C* **75** (2015) 313 [arXiv:1504.00317] [InSPIRE].

[34] V.N. Gribov and L.N. Lipatov, *Deep inelastic ep scattering in perturbation theory*, *Sov. J. Nucl. Phys.* **15** (1972) 438 [*Yad. Fiz.* **15** (1972) 781] [InSPIRE].

[35] Y.L. Dokshitzer, *Calculation of the structure functions for deep inelastic scattering and e^+e^- annihilation by perturbation theory in quantum chromodynamics*, *Sov. Phys. JETP* **46** (1977) 641 [*Zh. Eksp. Teor. Fiz.* **73** (1977) 1216] [InSPIRE].

[36] G. Altarelli and G. Parisi, *Asymptotic freedom in parton language*, *Nucl. Phys. B* **126** (1977) 298 [InSPIRE].

[37] R.K. Ellis and D.A. Ross, *The coupling of the QCD Pomeron in various semihard processes*, *Nucl. Phys. B* **345** (1990) 79 [InSPIRE].

[38] A. Colpani Serri et al., *Revisiting NLO QCD corrections to total inclusive J/ψ and Υ photoproduction cross sections in lepton-proton collisions*, arXiv:2112.05060 [InSPIRE].

[39] E.A. Kuraev, L.N. Lipatov and V.S. Fadin, *Multi-Reggeon processes in the Yang-Mills theory*, *Sov. Phys. JETP* **44** (1976) 443 [*Zh. Eksp. Teor. Fiz.* **71** (1976) 840] [InSPIRE].

[40] E.A. Kuraev, L.N. Lipatov and V.S. Fadin, *The Pomeranchuk singularity in non-Abelian gauge theories*, *Sov. Phys. JETP* **45** (1977) 199 [*Zh. Eksp. Teor. Fiz.* **72** (1977) 377] [InSPIRE].

[41] I.I. Balitsky and L.N. Lipatov, *The Pomeranchuk singularity in quantum chromodynamics*, *Sov. J. Nucl. Phys.* **28** (1978) 822 [*Yad. Fiz.* **28** (1978) 1597] [InSPIRE].

[42] S. Catani, M. Ciafaloni and F. Hautmann, *Gluon contributions to small x heavy flavor production*, *Phys. Lett. B* **242** (1990) 97 [InSPIRE].

[43] S. Catani, M. Ciafaloni and F. Hautmann, *High-energy factorization and small x heavy flavor production*, *Nucl. Phys. B* **366** (1991) 135 [InSPIRE].

[44] J.C. Collins and R.K. Ellis, *Heavy quark production in very high-energy hadron collisions*, *Nucl. Phys. B* **360** (1991) 3 [InSPIRE].

[45] S. Catani and F. Hautmann, *High-energy factorization and small x deep inelastic scattering beyond leading order*, *Nucl. Phys. B* **427** (1994) 475 [hep-ph/9405388] [INSPIRE].

[46] S. Catani, M. Ciafaloni and F. Hautmann, *Leptoproduction of heavy flavor at high energies*, *Nucl. Phys. B Proc. Suppl.* **29** (1992) 182 [INSPIRE].

[47] F. Hautmann, *Heavy top limit and double logarithmic contributions to Higgs production at m_H^2/s much less than 1*, *Phys. Lett. B* **535** (2002) 159 [hep-ph/0203140] [INSPIRE].

[48] R.V. Harlander, H. Mantler, S. Marzani and K.J. Ozeren, *Higgs production in gluon fusion at next-to-next-to-leading order QCD for finite top mass*, *Eur. Phys. J. C* **66** (2010) 359 [arXiv:0912.2104] [INSPIRE].

[49] S. Marzani and R.D. Ball, *High energy resummation of Drell-Yan processes*, *Nucl. Phys. B* **814** (2009) 246 [arXiv:0812.3602] [INSPIRE].

[50] G. Diana, *High-energy resummation in direct photon production*, *Nucl. Phys. B* **824** (2010) 154 [arXiv:0906.4159] [INSPIRE].

[51] R.D. Ball, V. Bertone, M. Bonvini, S. Marzani, J. Rojo and L. Rottoli, *Parton distributions with small-x resummation: evidence for BFKL dynamics in HERA data*, *Eur. Phys. J. C* **78** (2018) 321 [arXiv:1710.05935] [INSPIRE].

[52] xFITTER DEVELOPERS' TEAM collaboration, *Impact of low-x resummation on QCD analysis of HERA data*, *Eur. Phys. J. C* **78** (2018) 621 [arXiv:1802.00064] [INSPIRE].

[53] M.G. Echevarria, T. Kasemets, J.-P. Lansberg, C. Pisano and A. Signori, *Matching factorization theorems with an inverse-error weighting*, *Phys. Lett. B* **781** (2018) 161 [arXiv:1801.01480] [INSPIRE].

[54] Y.-Q. Ma and R. Venugopalan, *Comprehensive description of J/ψ production in proton-proton collisions at collider energies*, *Phys. Rev. Lett.* **113** (2014) 192301 [arXiv:1408.4075] [INSPIRE].

[55] Z.-B. Kang, Y.-Q. Ma and R. Venugopalan, *Quarkonium production in high energy proton-nucleus collisions: CGC meets NRQCD*, *JHEP* **01** (2014) 056 [arXiv:1309.7337] [INSPIRE].

[56] I. Balitsky, *Operator expansion for high-energy scattering*, *Nucl. Phys. B* **463** (1996) 99 [hep-ph/9509348] [INSPIRE].

[57] Y.V. Kovchegov, *Small x F_2 structure function of a nucleus including multiple Pomeron exchanges*, *Phys. Rev. D* **60** (1999) 034008 [hep-ph/9901281] [INSPIRE].

[58] I. Balitsky, *Factorization for high-energy scattering*, *Phys. Rev. Lett.* **81** (1998) 2024 [hep-ph/9807434] [INSPIRE].

[59] J. Jalilian-Marian, A. Kovner, A. Leonidov and H. Weigert, *The BFKL equation from the Wilson renormalization group*, *Nucl. Phys. B* **504** (1997) 415 [hep-ph/9701284] [INSPIRE].

[60] J. Jalilian-Marian, A. Kovner, A. Leonidov and H. Weigert, *The Wilson renormalization group for low x physics: towards the high density regime*, *Phys. Rev. D* **59** (1998) 014014 [hep-ph/9706377] [INSPIRE].

[61] J. Jalilian-Marian, A. Kovner and H. Weigert, *The Wilson renormalization group for low x physics: gluon evolution at finite parton density*, *Phys. Rev. D* **59** (1998) 014015 [hep-ph/9709432] [INSPIRE].

[62] E. Iancu, A. Leonidov and L.D. McLerran, *The renormalization group equation for the color glass condensate*, *Phys. Lett. B* **510** (2001) 133 [hep-ph/0102009] [INSPIRE].

[63] E. Iancu, A. Leonidov and L.D. McLerran, *Nonlinear gluon evolution in the color glass condensate. 1*, *Nucl. Phys. A* **692** (2001) 583 [hep-ph/0011241] [INSPIRE].

[64] B.L. Ioffe, V.S. Fadin and L.N. Lipatov, *Quantum chromodynamics perturbative and nonperturbative aspects*, Cambridge University Press, Cambridge, U.K. (2010).

[65] Y.V. Kovchegov and E. Levin, *Quantum chromodynamics at high energy*, Cambridge University Press, Cambridge, U.K. (2012) [INSPIRE].

[66] V. Del Duca, *An introduction to the perturbative QCD Pomeron and to jet physics at large rapidities*, hep-ph/9503226 [INSPIRE].

[67] J.C. Collins, *Foundations of perturbative QCD*, Cambridge University Press, Cambridge, U.K. (2009).

[68] M. Nefedov, *Sudakov resummation from the BFKL evolution*, *Phys. Rev. D* **104** (2021) 054039 [arXiv:2105.13915] [INSPIRE].

[69] M. Hentschinski, *Transverse momentum dependent gluon distribution within high energy factorization at next-to-leading order*, *Phys. Rev. D* **104** (2021) 054014 [arXiv:2107.06203] [INSPIRE].

[70] L.N. Lipatov, *Gauge invariant effective action for high-energy processes in QCD*, *Nucl. Phys. B* **452** (1995) 369 [hep-ph/9502308] [INSPIRE].

[71] B.A. Kniehl, V.A. Saleev and D.V. Vasin, *Bottomonium production in the Regge limit of QCD*, *Phys. Rev. D* **74** (2006) 014024 [hep-ph/0607254] [INSPIRE].

[72] Z.-G. He, B.A. Kniehl, M.A. Nefedov and V.A. Saleev, *Double prompt J/ψ hadroproduction in the parton reggeization approach with high-energy resummation*, *Phys. Rev. Lett.* **123** (2019) 162002 [arXiv:1906.08979] [INSPIRE].

[73] P. Hagler, R. Kirschner, A. Schafer, L. Szymanowski and O. Teryaev, *Heavy quark production as sensitive test for an improved description of high-energy hadron collisions*, *Phys. Rev. D* **62** (2000) 071502 [hep-ph/0002077] [INSPIRE].

[74] P. Hagler, R. Kirschner, A. Schafer, L. Szymanowski and O.V. Teryaev, *Towards a solution of the charmonium production controversy: k^- perpendicular factorization versus color octet mechanism*, *Phys. Rev. Lett.* **86** (2001) 1446 [hep-ph/0004263] [INSPIRE].

[75] B.A. Kniehl, D.V. Vasin and V.A. Saleev, *Charmonium production at high energy in the k_T-factorization approach*, *Phys. Rev. D* **73** (2006) 074022 [hep-ph/0602179] [INSPIRE].

[76] T. Jaroszewicz, *Gluonic Regge singularities and anomalous dimensions in QCD*, *Phys. Lett. B* **116** (1982) 291 [INSPIRE].

[77] R. Kirschner and M. Segond, *Small x resummation in collinear factorisation*, *Eur. Phys. J. C* **68** (2010) 425 [arXiv:0910.5443] [INSPIRE].

[78] A. Vogt, S. Moch and J.A.M. Vermaseren, *The three-loop splitting functions in QCD: the singlet case*, *Nucl. Phys. B* **691** (2004) 129 [hep-ph/0404111] [INSPIRE].

[79] T. Lukowski, A. Rej and V.N. Velizhanin, *Five-loop anomalous dimension of twist-two operators*, *Nucl. Phys. B* **831** (2010) 105 [arXiv:0912.1624] [INSPIRE].

[80] B.A. Kniehl, V.A. Saleev, A.V. Shipilova and E.V. Yatsenko, *Single jet and prompt-photon inclusive production with multi-Regge kinematics: from Tevatron to LHC*, *Phys. Rev. D* **84** (2011) 074017 [arXiv:1107.1462] [INSPIRE].

[81] J. Blumlein, *On the k_T dependent gluon density of the proton*, in 3$^{\rm rd}$ *workshop on Deep Inelastic Scattering and QCD (DIS 95). Proceedings, workshop, Paris, France,* 24–28 *April* 1995, DESY 95-121, (1995), p. 265 [hep-ph/9506403] [INSPIRE].

[82] T.-J. Hou et al., *New CTEQ global analysis of quantum chromodynamics with high-precision data from the LHC*, *Phys. Rev. D* **103** (2021) 014013 [arXiv:1912.10053] [INSPIRE].

[83] S. Bailey, T. Cridge, L.A. Harland-Lang, A.D. Martin and R.S. Thorne, *Parton distributions from LHC, HERA, Tevatron and fixed target data: MSHT20 PDFs*, *Eur. Phys. J. C* **81** (2021) 341 [arXiv:2012.04684] [INSPIRE].

[84] NNPDF collaboration, *Parton distributions from high-precision collider data*, *Eur. Phys. J. C* **77** (2017) 663 [arXiv:1706.00428] [INSPIRE].

[85] A. Buckley et al., *LHAPDF6: parton density access in the LHC precision era*, *Eur. Phys. J. C* **75** (2015) 132 [arXiv:1412.7420] [INSPIRE].

[86] R.K. Ellis, F. Hautmann and B.R. Webber, *QCD scaling violation at small x*, *Phys. Lett. B* **348** (1995) 582 [hep-ph/9501307] [INSPIRE].

[87] G. Altarelli, R.D. Ball and S. Forte, *Resummation of singlet parton evolution at small x*, *Nucl. Phys. B* **575** (2000) 313 [hep-ph/9911273] [INSPIRE].

[88] J.L. Albacete and C. Marquet, *Gluon saturation and initial conditions for relativistic heavy ion collisions*, *Prog. Part. Nucl. Phys.* **76** (2014) 1 [arXiv:1401.4866] [INSPIRE].